15434

WT-917 (EX)

EXTRACTED VERSION

OPERATION CASTLE

Project 2.6a
Chemical, Physical, and Radiochemical Characteristics of the Contaminant

Pacific Proving Grounds
March — May 1954

Headquarters Field Command
Armed Forces Special Weapons Project
Sandia Base, Albuquerque, New Mexico

September 1955

NOTICE

This is an extract of WT-917, Operation CASTLE, Project 2.6a, which remains classified SECRET/RESTRICTED DATA as of this date.

Extract version prepared for:

Director
DEFENSE NUCLEAR AGENCY
Washington, D.C. 20305

15 May 1981

GENERAL SHOT INFORMATION

	Shot 1	Shot 2	Shot 3	Shot 4	Shot 5	Shot 6
DATE	1 March	27 March	7 April	26 April	5 May	14 May
CODE NAME (Unclassified)	Bravo	Romeo	Koon	Union	Yankee	Nectar
TIME*	06:40	06:25	06:15	06:05	06:05	06:15
LOCATION	Bikini, West of Charlie (Namu) on Reef	Bikini, Shot 1 Crater	Bikini, Tare (Eninman)	Bikini, on Barge at Intersection of Arcs with Radii of 6900' from Dog (Yurochi) and 3 Statute Miles from Fox (Aomoen).		Eniwetok, IVY Mike Crater, Flora (Elugelab)
TYPE	Land	Barge	Land	Barge	Barge	Barge
HOLMES & NARVER COORDINATES	N 170,617.17 E 76,163.98	N 170,635.05 E 75,950.46	N 100,154 50 E 109,799.00	N 161,698 83 E 116,800.27	N 161,424 43 E 116,688,15	N 147,750.00 E 67,790.00

* APPROXIMATE

ABSTRACT

The bomb debris from surface, land and water shots at Operation CASTLE was studied to determine the physical, chemical, and radiochemical characteristics.

The fallout from the surface land shots consisted chiefly of irregular white particles 25 μ to 2 mm in diameter. They were derived from coral and had the radioactivity concentrated near their surfaces. About 5 per cent of the activity in the solid fallout was water soluble; 95 per cent dissolved in dilute acetic acid. The fallout from the surface water shots was invisible both in the air and after it had deposited. It was collected on special filters and on a film by electrostatic precipitation. The filters and film and their autoradiographs were studied microscopically. These studies showed that the fallout consisted of microscopic solid crystals and small droplets. The autoradiographs indicated the presence on the filters of many particles which were invisible under the microscope. The major part of the radioactivity was associated with crystalline aggregates and droplets up to about 2 mm in diameter. Water dissolved from 60 to 90 per cent of the radionuclides from this type of fallout.

Fallout and cloud samples from land and water shots were analyzed chemically for major constituents and trace elements including many of the radionuclides. Coral and sea water contributed the major constituents, bomb products being present in trace concentrations. Radiochemical analysis showed the valley of the fission product yield curve was about 20 times higher and the heavy wing at mass 156 about 6 times higher than the yield curve from thermal neutrons on U^{235}. The important induced radionuclides were U^{239}-Np^{239}, U^{237}, and U^{240}. The presence of these had a marked effect on the decay curves and energy spectra especially at intermediate times after detonation. The neptunium was distributed between oxidation states; iodine occurred principally as iodide.

The information obtained from these studies has aided in (a) an understanding of the mechanism of formation of the fallout, (b) assessing the radiological situation in fallout areas, (c) synthesizing simulants for laboratory studies, and (d) interpreting data obtained in proof tests of countermeasures for ships.

CHAPTER 1

INTRODUCTIONS

Radiation fields produced by fallout from a nuclear detonation create debilitating effects far beyond the range of its blast damage. Information on transport and distribution of fallout and knowledge of its physical, chemical, and radiochemical properties are prerequisite to development of countermeasures against its radiation fields. At Operation CASTLE the transport and distribution of fallout was principally the concern of Projects 2.5a and 6.4; Project 2.5b studied the fallout on islands near the shot point; investigation of fallout properties was the concern of Projects 2.6a and 2.6b.

1.1 OBJECTIVES AND BACKGROUND

The purpose of Project 2.6a was to investigate the chemical, physical, and radiochemical properties of the fallout for:

a. Deducing the mechanism whereby contaminant is formed.

b. Assessing radiological situations.

c. Specifying realistic simulants of radiological contaminants for use in contamination and decontamination tests.

d. Interpreting the data obtained in proof testing atomic warfare countermeasures for ships.

1.1.1 Mechanism of Contamination Formation

The contamination formed from surface or sub-surface detonation of a nuclear weapon has important military consequences. It was found at Operations CROSSROADS,[8] JANGLE,[17] and IVY[12] that high levels of surface contamination were produced as a result of surface or sub-surface detonations. Each of these operations represented a unique condition of detonation, but provided insufficient data to establish bases for predicting radiological effects for a wide range of probable conditions of detonation. An understanding of the mechanism whereby contamination is produced is necessary in making such predictions. Data obtained in CASTLE are applicable in answering such questions on the mechanics of the event as: To what extent is wet contaminant formed by condensation phenomena? With what type of particles do the primary particles of

radioactive debris associate? What is the rate and extent of settling out and mixing of fallout deposited on the water surface?

Owing to the incompleteness of the data taken at Shot Baker, CROSSROADS, essentially nothing was known prior to CASTLE concerning the mechanism of formation of wet contamination from this type of burst. The relative contributions of base surge and fallout were uncertain; the roles of condensation, evaporation and mixing with sea water in the production of either base surge or fallout were unknown. Particle size and individual particle studies undertaken at JANGLE and IVY have yielded considerable information on the mechanism of formation, dispersion and reactions of dry contaminants from these operations.[25,20,1,2]

1.1.2 Assessment of Radiological Situations

Extensive laboratory contamination-decontamination programs have been undertaken to solve presumed field radiological problems but in many cases lack of full-scale test data has made it impossible to define them clearly. For example, before CASTLE it had not been determined whether an internal contamination hazard would be produced on ships by radioactive aerosols from an underwater detonation, because the nature of such aerosols was unknown; the relative contribution of gamma radiation from fallout in the water with that on contaminated ships could not be calculated because the rate of settling or mixing of the contaminant in the water was unknown. Insoluble particles will settle depending on size and density while dissolved (ionic) contaminants will mix; colloidal material, if present, will mix and settle slowly. The assessment of such radiological situations and the development of countermeasures require a knowledge of many physical and chemical properties of the contaminant.

Limited data exist with regard to the contaminants which may be produced by surface and underground detonations because of the atypical nature of the soils at IVY and JANGLE. No direct information has been obtained on the nature of contaminants from underwater detonations. For this reason, there is special interest in surface water shots which should produce a contaminant most similar in nature to that from an underwater detonation.

1.1.3 Specifications of Simulants for Radiological Contaminants

If meaningful laboratory contamination-decontamination results are to be obtained, it is essential that the artificial contaminants used must simulate real ones in chemical and radiochemical composition and in important chemical and physical characteristics. In the past, the radiochemical composition of artificial contaminants [14] has been based upon yields of various radioelements from slow fission of U^{235}. It is important to know the extent of difference in fission yields for nuclear processes other than slow fission and whether induced activities contribute appreciably to the contamination. Finally, it is necessary to evaluate the relative contribution of each radioelement to contamination fields on the basis of its yield and the number and energy of the gamma rays emitted by the various radionuclides of that element.

Fission yield curves have been determined for various fission weapons detonated to date. Although some such information exists for the fusion-fission device detonated at IVY, it was necessary to determine the important radionuclides produced by the detonation of new types of devices at CASTLE.

The presence of activities induced in elements found in sea water was reported for Shot Baker at CROSSROADS. An analysis for induced activities was also made at JANGLE.[19,4] It was shown that the single important induced activity present in JANGLE fallout any time during the first 90 days after detonation was Np^{239}, formed from U^{238} present in the device. No important induced activities have been reported for IVY. However, some unconfirmed data indicated an activity present in high yield at early times.[12] Detonation of certain of the CASTLE devices over water posed the question of the extent to which important induced activities would be formed under these conditions.

Calculations for estimating the contribution of different chemical elements to the rate of gamma radiation have been made. Yields from slow neutron fission were used. Data regarding the number and energy of the gamma rays emitted by various radionuclides were incomplete. To improve the validity of these important calculations better radionuclide yield data were required. Also it was important to measure the gamma energies of a few radionuclides, for which the energies had not been adequately defined.

It has been shown that contamination-decontamination behavior is a function of the physical and chemical properties of the contaminant system. This is illustrated by the ease with which gross particulate contaminants are removed,[32] by the relation of particle size to decontamination efficiency,[18] and by the influence which composition and oxidation state of liquid contaminants exert on decontamination effectiveness.[22,23,24,10] Definition of the real contaminant system was therefore an important prerequisite for specification of contaminant simulants.

Definition of any chemical system requires a knowledge of the identity and amounts of its various components. The contaminating fallout from each shot consists largely of nonradioactive materials. The production of realistic laboratory contaminants for more basic information about radiological decontamination has, in the past, suffered severely from the absence of elementary information about the actual contamination-decontamination system in question. Since real contamination had not been available, many investigations were conducted using highly questionable contamination procedures with no available means of relating the data to real events. Knowledge of the concentrations of macro constituents along with radiochemical analytical data provide all the information needed to prepare laboratory contaminants which would consistently have the same general decontamination characteristics. With such added information as field isodose data in conjunction with isoconcentration plots from these data, laboratory experiments on the effect of level on decontamination can be investigated reliably.

The thermodynamic states of inactive or bulk materials usually are of greater importance than those of the radioactive constituents. It is inconceivable, for any radiological contamination of interest,

that the radioactive constituents can comprise as much as 0.01 per cent of the total fallout. Hence, most of the properties of the contaminant except the radiation characteristics will be essentially determined by the inactive elements. Therefore, emphasis was placed on determining the states of the inactive constituents and the states of a few important gamma emitting elements.

1.1.4 Proof Testing Atomic Warfare Countermeasures for Ships

There has been extensive laboratory and field scale development work on atomic warfare (AW) countermeasures for ships.5/ Project 6.4 tested the washdown system at CASTLE and conducted decontamination operations on the ships used in the operation. Since the contamination found from certain of the shots of CASTLE differed from either real or simulated contaminants previously studied, detailed knowledge of the properties of the contaminant was needed for interpreting these results.

Information on the rate of radioactive decay, gross gamma energy spectrum, and the ratio of beta to gamma radiation was furnished by Project 2.6a.

TABLE 3.5 - Physical State Fractionation of Gamma Activity

Sample	Time After Detonation (days)	Wt.of Solid (%)	pH	Gamma Count			Amount Ionic(a) in Liquid Phase (%)
				Solid (%)	Ionic (%)	Colloidal (%)	
1-251.03	6.5	9.2	11.9	96.33	3.56	0.11	97.0
1-251.02	8.1	0.94	12.3	92.08	7.72	0.20	97.5
1-250.05	8.3	0.85	9.0	98.05	1.89	0.06	97.0
2-A4	3.4	< 0.01	7.5	24.70	72.90	2.40	96.8
3-Coca TC	4.2	0.18	10.5	92.44	7.33	0.23	97.0
3-251.02	5.5	0.23	11.2	94.17	5.60	0.23	96.1
4-Y39	1.8	< 0.01	7.7	40.20	57.91	1.89	96.8

(a) Percentage of gamma count in the liquid phase found in the ionic fraction

TABLE 3.6 - Summary, Physical State Fractionation of Gamma Activity

Shot Type	Shot Number	Number of Samples	Time After Detonation (days)	Wt.of Solid (%)	pH	Gamma Count			Amt.Ionic(a) in Lqd.Phase (%)
						Solid (%)	Ionic (%)	Colloidal (%)	
Island	1	3	6.5-8.3	0.85-9.2	9.0-12.3	92.1-98.1	1.9-7.7	0.06-0.2	97.0-97.5
	3	2	4.2-5.5	0.18-0.23	10.5-11.2	92.4-94.2	5.6-7.3	0.23-0.23	96.1-97.0
Barge	2	1	3.4	< 0.01	7.5	24.7	72.9	2.4	96.8
	4	1	1.8	< 0.01	7.7	40.2	57.9	1.9	96.8

(a) Percentage of gamma count in the liquid phase found in the ionic fraction

TABLE 3.8 - Gamma Energy Distribution of Physical State Fractions Determined by Lead Absorption

Sample[b]	Time (days)	Half-thickness (gm of Pb/sq cm)	Fraction of Total Count			Average Energy (kev)
			Energy (kev)	(Uncorrected) (%)	(Corrected)[a] (%)	
1-251.03 S	8.3	0.27	150.	71.7	50.1	
		1.42	340.	16.8	21.5	466.
		11.0	1120.	11.5	28.4	
1-251.03 F	8.3	0.27	150.	60.8	36.3	
		1.85	380.	18.5	19.35	669.
		11.7	1220.	20.7	44.35	
1-251.03 C	8.3	0.38	180.	41.2	18.25	
		2.90	480.	18.8	17.95	1153.
		14.1	1620.	40.0	63.8	
1-251.02 S	9.1	0.25	145.	69.9	47.0	
		1.52	350.	17.3	21.9	527.
		11.8	1230.	12.8	31.1	
1-251.02 F	9.1	0.30	160.	73.4	50.25	
		1.73	375.	13.0	17.35	508.
		11.0	1120.	13.6	32.4	
1-251.02 C	9.1	0.38	180.	44.7	21.8	
		2.04	400.	20.5	19.6	880.
		12.3	1300.	34.8	58.6	
1-250.05 S	9.2	0.27	150.	73.2	53.7	
		1.32	325.	18.0	23.2	429.
		11.5	1180.	8.8	23.1	

(a) Corrected for counter efficiency as function of energy
(b) State of sample indicated by following symbols:
S = solid; F = ultrafiltrate (ionic); C = colloid

TABLE 3.8 - Gamma Energy Distribution of Physical State Fractions Determined by Lead Absorption (Contd.)

Sample[b]	Time (days)	Half-thickness (gm of Pb/sq cm)	Fraction of Total Count			Average Energy (kev)
			Energy (kev)	(Uncorrected) (%)	(Corrected)[a] (%)	
1-250.05 F	9.2	0.34	170.	70.6	46.1	
		2.96	485.	15.4	22.15	573.
		11.7	1220.	14.0	31.75	
1-250.05 C	9.2	0.32	163.	48.5	26.1	
		1.27	320.	24.2	22.3	723.
		11.5	1180.	27.3	51.6	
2-A4 S	3.6	0.27	150.	66.2	44.0	
		1.40	340.	19.4	23.5	478.
		10.1	1020.	14.4	32.5	
2-A4 F	3.6	0.27	150.	75.9	57.25	
		1.40	340.	16.9	23.3	390.
		11.3	1160.	7.25	19.45	
2-A4 C	3.6	0.27	150.	63.4	40.5	
		1.40	340.	21.0	24.5	529.
		10.8	1100.	15.6	35.0	
2-A4 S	5.3	0.25	145.	68.0	46.0	
		1.40	340.	18.7	23.2	463.
		10.2	1030.	13.3	30.8	
2-A4 F	5.3	0.25	145.	73.3	53.6	
		1.40	340.	18.7	25.15	433.
		12.1	1270.	8.0	21.25	
2-A4 C	5.3	0.25	145.	65.7	42.5	
		1.40	340.	18.7	22.25	514.5
		10.6	1070.	15.6	35.25	

fraction was higher than that of the ionic fraction so that the average energy for the solid fraction was higher than for the Shot 1 samples. The absorption curve of the colloidal fraction was again the highest of the three resulting in a highest average energy for the colloidal fractions.

Gamma spectra were taken of samples for Shots 2,3, and 4, but because of low resolution and other limitations, it was not possible to use the gamma-spectra to obtain important information about the constituents of the physical state fractions.

In general, the spectra only support what was already obvious, such as the fact that Np^{239}, which was the most important single contributor to the activity in the time range 2 to 10 days, became less important at later times.

Figure 3.8 is a gamma analyzer plot for pure neptunium separated from the fallout sample 3-251.02. It was taken 7 days after detonation. In the range 0 to 0.7 Mev, it shows the reported Np^{239} peaks at 0.065, 0.105, 0.230, and 0.295 Mev.

Figures 3.9 through 3.11 are gamma analyzer spectra (low energy region) for the physical state fraction of the same sample at the same time. The solid fraction spectrum, which contained 94 per cent of the activity was a fair reproduction of the neptunium spectrum with an additional peak at 0.51 Mev due to an unknown constituent. The ultrafiltrate fraction, however, did not reproduce the neptunium spectrum; the spectrum had peaks at 0.14, 0.39, and 0.49 Mev. The peaks at about 0.5 Mev are undoubtedly due largely to annihilation gammas, indicating the presence of gamma radiation with energies greater than 1 Mev. The colloidal fraction spectrum appeared to contain portions of the neptunium spectrum, as well as peaks found in the other fractions. Spectra of fractions taken at other times show other peaks, but it was not possible to identify these in the absence of other information about important species present.

3.2.2.4 Quantitative Analysis of Physical State Fractions

The concentration analysis of the solid and ionic fractions (as separated in the field) is given in Table 3.9. Aliquots of the solid and the ionic fractions of samples 2-A4, 3-Coca TC, 3-251.02 and 4-Y39 were returned to the laboratory as liquids (the solid fraction had been dissolved in HCl and made up to 100 ml). The concentrations are given in micrograms per milliliter (ppm). The colloidal fraction was not returned for analysis because it was used in its entirety as a counting sample and because of the difficulty of recovering the small quantities from the ultrafilter membrane. There were no visible deposits on the membrane.

Table 3.10 gives the mass in milligrams of each element in the liquid and solid fractions of the total sample recovered in the field. It also gives the total mass of each element in the total original sample as well as the percentage distribution of each element between the liquid and the solid fractions. For sample 2-A4, the liquid fraction data are taken as the average of the supernatant and ultrafilter data. For the other samples the ultrafiltrate represents the liquid; supernatant was not returned for analysis.

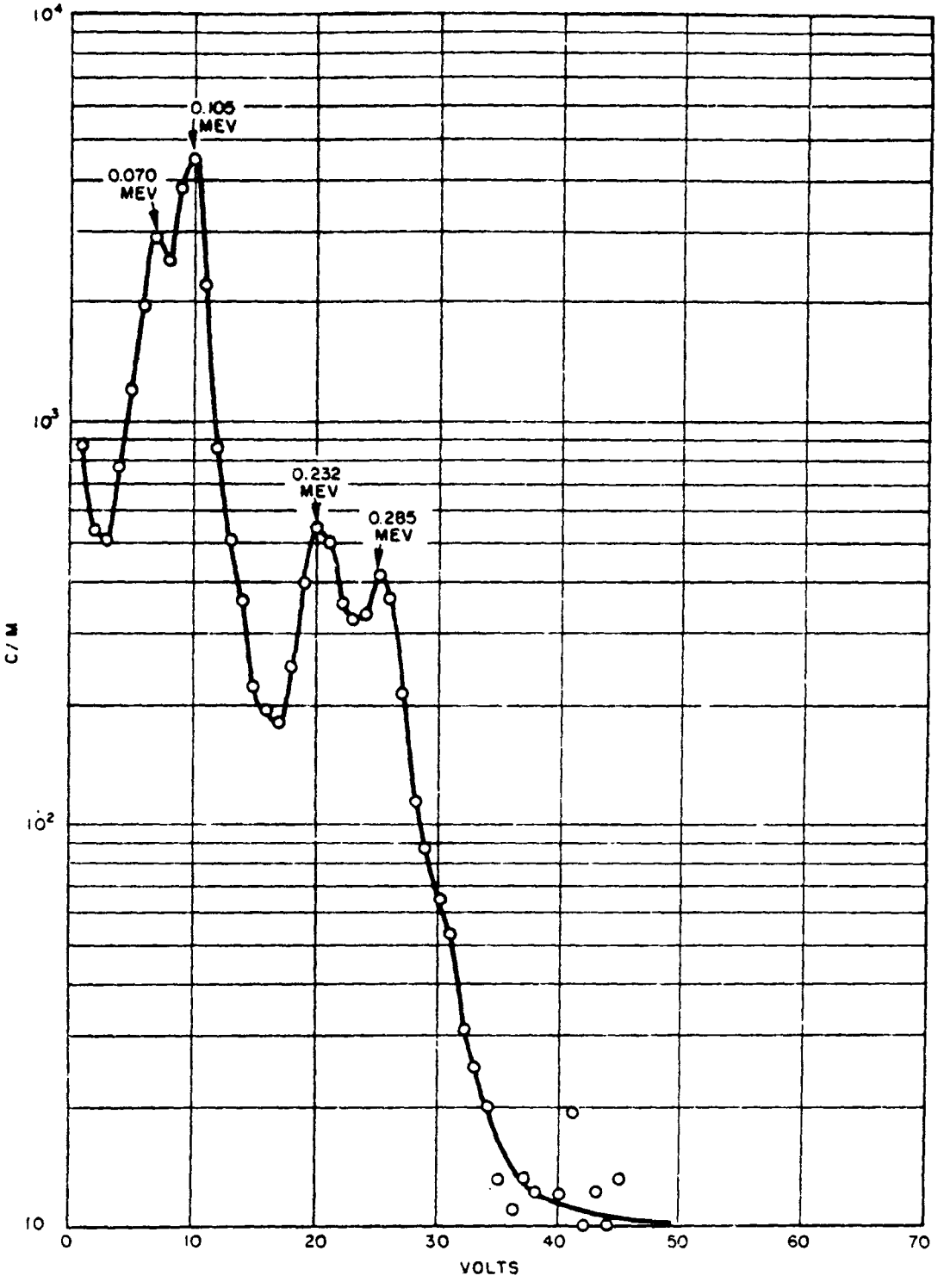

Fig. 3.8 Gamma Spectra of NpV-VI, Sample 3-251.02 at + 7 days

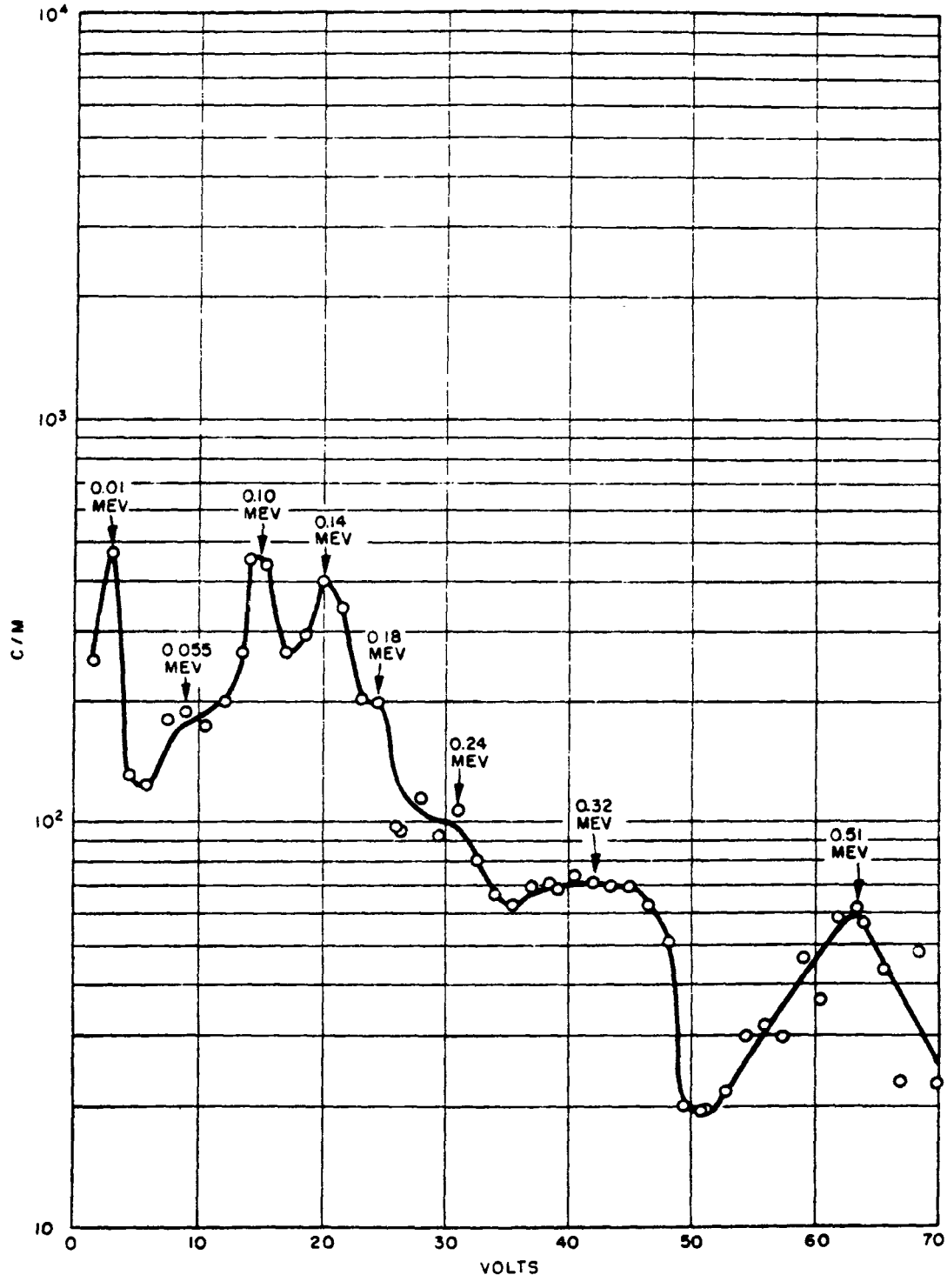

Fig. 3.9 Gamma Spectra of Solid,
Sample 3-251.02 at + 7 days

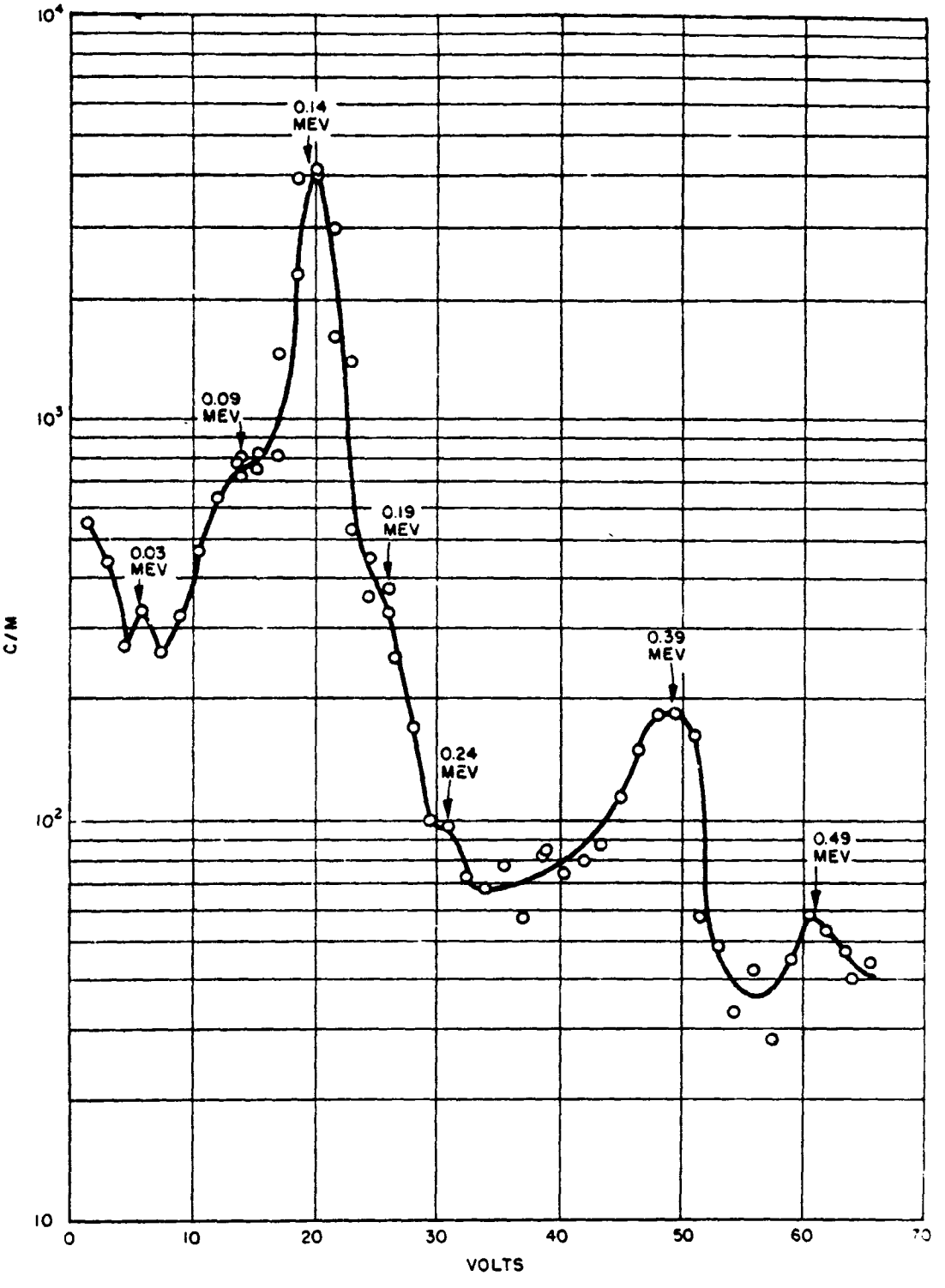

Fig. 3.10 Gamma Spectra of Ultrafiltrate, Sample 3-251.02 at + 7 days

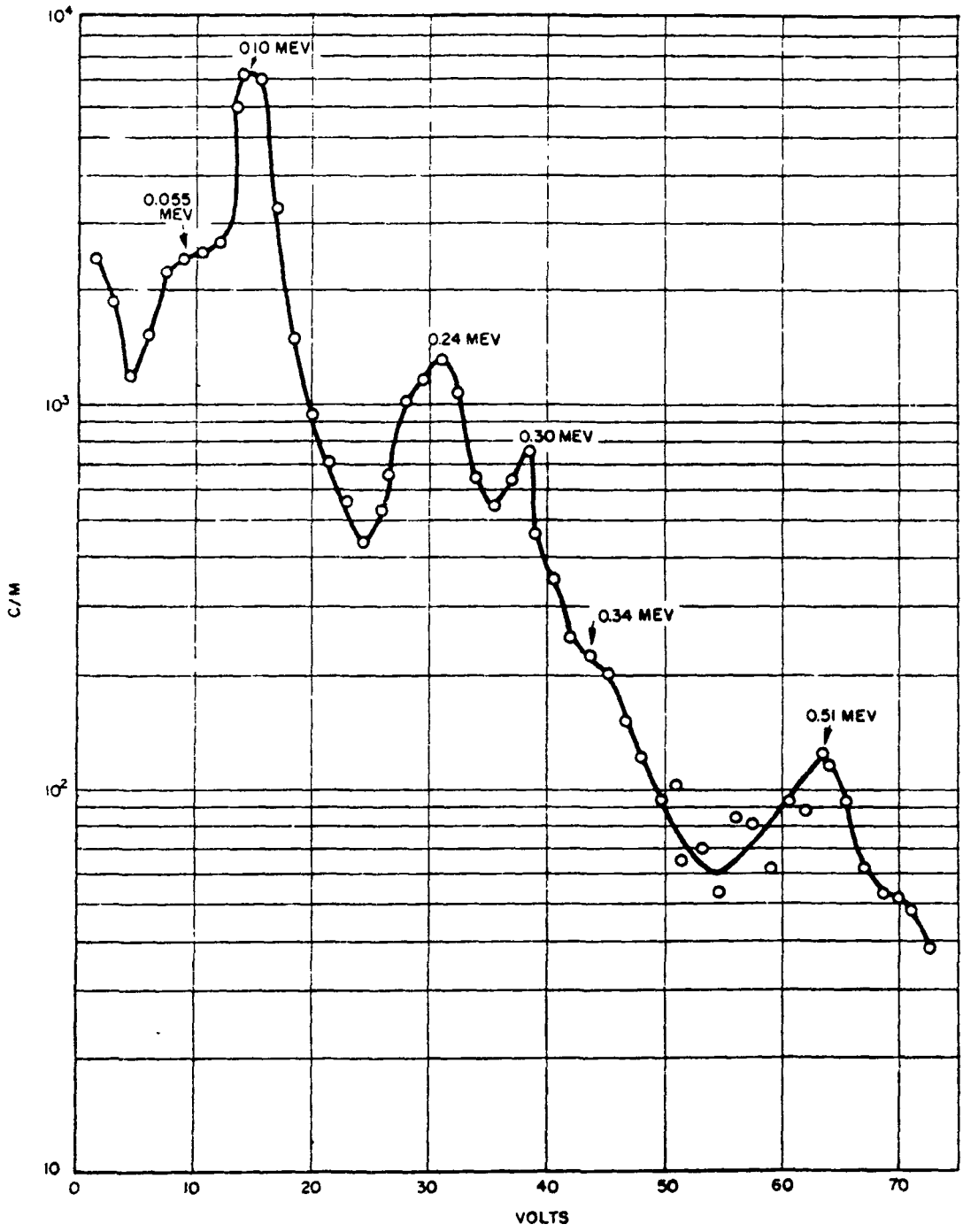

Fig. 3.11 Gamma Spectra of Colloid Fraction, Sample 3-251.02 at + 7 days

TABLE 3.9 - Concentration of Elements of Interest in Solutions of Physical State Fractions

Sample	Vol. of Sample separated in field, (ml)	Vol. of Sample as analyzed, (ml)	Concentration (μg/ml)								
			Cl[a]	Na	K	Mg	Ca	Fe	Al	Cu	Si
2-A4											
Supernate		8.2	1,595.	840.	37.0	104.	58.6	0.78	<0.40	<0.40	0.97
Ultrafiltrate	19.3	3.5	355.	574.	39.6	151.	105.	<0.4	<0.8	<7.6	<2.0
Solid		100.4	-	1.5	1.8	0.0	7.6	2.74	0.40	0.22	0.03
3-Coca TC											
Ultrafiltrate	12.1	2.7	1,170.	227.	11.5	28.0	428.	<0.3	<0.67	<0.43	<0.40
Solid		99.0	-	0.8	0.0	4.8	79.	1.50	0.30	<0.08	0.02
3-251.02											
Ultrafiltrate	27.0	7.4	35.5	37.3	1.7	0.0	15.8	0.67	0.02	<0.38	1.10
Solid		98.4	-	1.6	0.0	15.2	158.	1.09	0.30	<0.08	0.05
4-Y39											
Ultrafiltrate	15.0	4.0	25,100.	12,680.	496.	1,870.	574.	<0.05	1.15	<0.76	1.84
Solid		99.0	-	0.0	0.0	0.0	4.8	0.55	0.02	<0.08	0.03

(a) Chloride concentrations given originally as normality; for <400 μg/ml, only 1 significant figure
400 - 4000 μg/ml 2 significant figures
>4000 μg/ml 3 significant figures

Table 3.10 - Mass Distribution of Elements of Interest in Liquid and Solid Fractions

Sample		Cl		Na		K		Mg		Ca	
		mg	%	mg	%	mg	%	mg	%	mg	%
2-A4	Liquid	63.0	100	28.0	98.9	1.49	80.1	5.04	100.	3.23	67.6
(39.5 ml)	Solid	-	-	0.31	1.1	0.37	19.9	0.00	0.	1.55	32.4
	Total	63.0		28.3		1.86		5.04		4.78	
3-Coca TC	Liquid	419.	100	81.1	97.1	4.10	100.	10.0	41.4	153.0	39.7
(355. ml)	Solid	-	-	2.4	2.9	0.00	0.	14.2	58.6	233.0	60.3
	Total	419.		83.5		4.10		24.2		386.0	
3-251.02	Liquid	43.	100	43.4	86.3	1.97	100.	0.00	0.	18.3	2.6
(1160 ml)	Solid	-	-	6.9	13.7	0.00	0.	64.0	100.	679.	97.4
	Total	43.		50.3		1.97		64.0		697.	
4-Y39	Liquid	1,615.	100	815.	100.	31.9	100.	120.0	100.	36.9	94.6
(64.4 ml)	Solid	-	-	0.00	0.	0.00	0.	0.00	0.	2.06	5.4
	Total	1,615		815.		31.9		120.0		39.0	

TABLE 3.10 - Mass Distribution of Elements of Interest in Liquid and Solid Fractions (Continued)

Sample		Fe		Al		Cu		Si	
		mg	%	mg	%	mg	%	mg	%
2-A4	Liquid	< 0.047	< 8.	< 0.047	< 36.	< 0.016	< 26.	0.038	86.
(39.5 ml)	Solid	0.560	> 92.	0.082	> 64.	0.045	> 74	0.006	14.
	Total	0.560		0.082		0.045		0.044	
3-Coca TC	Liquid	< 0.11	< 2.	< 0.24	< 21.	< 0.15	-	< 0.14	< 70.
(355. ml)	Solid	4.40	> 98.	0.88	> 79.	< 0.24	-	0.06	> 30.
	Total	4.40		0.88		< 0.39		0.06	
3-251.02	Liquid	0.776	14.4	0.0232	1.8	< 0.44	-	1.16	84.0
(1160. ml)	Solid	4.60	85.6	1.3	98.2	< 0.34	-	0.22	16.0
	Total	5.38		1.32		< 0.78		1.38	
4-Y39	Liquid	< 0.003	< 1.	0.0741	89.3	< 0.049	-	0.119	90.2
(64.4 ml)	Solid	0.236	> 99.	0.0086	10.7	< 0.034	-	0.013	9.8
	Total	0.236		0.083		< 0.083		0.0132	

Since the concentrations for many of the elements were extremely low and the volumes of the ultrafiltrate were small, some of the analyses had to be made near or below their lower limit of reliability. Thus, the results for iron, aluminum, and copper, which are the important detonation products, are very much in doubt. However, some conclusions can be drawn. Sodium and potassium, as expected, are predominantly in the liquid fraction. Magnesium and calcium, derived from both sea water and coral, are predominantly in the liquid fraction in the barge shot samples and predominantly in the solid fraction in the island shot samples. Calcium hydroxide being more insoluble than magnesium as well as constituting a larger percentage of coral had a greater tendency to be in the solid fraction than does magnesium.

More than 85 per cent of the iron was always found in the solid fraction. Aluminum also was found predominantly in the solid fraction; however, lower total concentrations of aluminum and lower pH tend to reverse this behavior.

3.3 CHEMICAL STATE OF NEPTUNIUM AND IODINE

Experiments were carried out to determine the oxidation states of Np and I in the fallout material. These two elements contribute significantly to the gamma radiation of the fallout from nuclear detonations, and accordingly, their contamination-decontamination behavior is important. Furthermore, the decontamination of these two elements depends on their oxidation states since the sorption and solubility and chemical reactivity of each are dependent on it. Knowledge of the chemical behavior of a few of the important radionuclides in the fallout together with that of some of the stable elements could lead to a realistic and practical approach to the preparation of synthetic contaminants.

3.3.1 Oxidation State of Neptunium

The oxidation state of Np in fallout samples was determined for Shots 1 through 4. In order to carry out the determination, a fairly large amount of activity was required (sample reading of 20 to 30 mr/hr at surface of container).

3.3.1.1 Chemical Treatment of Samples

The procedure for separating Np(IV) from Np(V) and Np(VI) was based on the extraction of Np(IV) into a 0.4 M TTA solution in benzene from a 2N-HCl aqueous phase. The Np(IV) back-extracts into an aqueous phase of 8N-HCl. The chemical procedure is given in Appendix A.

3.3.1.2 Neptunium Results

The experimental results for Shots 1,2,3, and 4 are tabulated in Table 3.11.

Two Shot 1 samples not listed in Table 3.11 were processed but the results were not considered satisfactory for the reasons given below.

Shot 1 sample 251.02 (land station) was the first processed. As a result of the observations from that experiment, significant improvements were made in the procedure. Therefore, the results of that run, which gave 10 per cent Np(IV) and 90 per cent Np(V-VI), were not considered significant. On sample 251.04, Shot 1, an attempt was made to shorten the neptunium procedure considerably by eliminating some of the purification steps. However, decay curves of the product indicated impure neptunium which invalidated the results.

TABLE 3.11 - Summary of Analysis of Neptunium Oxidation States

Shot	Station	Np(IV) (%)	Np(V-VI) (%)	Sample Source
1	1-250.05	58	42	Lagoon station
2	2-T4	44	56	Free floating buoy
3	3-Coca TC	66	34	Center of lagoon
3	3-251.02	80	20	Island station
4	4-Y39	77	23	YAG-39
	Average	65 ± 11	35 ± 11	

The decay of the various neptunium fractions for all samples was followed for at least three half-lives. In every case, except those specified above, the neptunium showed no indication of any impurities. Decay was followed with a gamma scintillation counter. Gamma ray spectrometer data were also used to help identify the Np samples.

3.3.2 Chemical State of Iodine

The chemical state of iodine in the fallout samples was determined for Shots 1 through 4. The procedures and results are given in the following sections.

3.3.2.1 Chemical Treatment of Samples

Several procedures were used to investigate the oxidation and phase state of iodine in the fallout material. In the first procedure, $BaCl_2$ was added to the original sample to precipitate the sea water sulfate and any iodate present as $BaIO_3$. The sample was centrifuged to separate the solid and liquid phases. Iodide and iodate carriers were added to the supernatant and precipitate, respectively, and the iodine oxidized and reduced with $NaNO_2$ and Na_2SO_3 alternately while in contact with a CCl_4 phase to extract the iodine as I_2. This procedure actually gave the amount of iodine in the liquid and solid phases when the two were initially present (as was the case in the samples as received for Shots 1 and 3).

In another procedure, the sample was dissolved in a minimum amount of HCl, divided into two aliquots. Iodide carrier was added to

one fraction and iodate carrier to the other. The iodide carrier was oxidized with $NaNO_2$ in contact with a CCl_4 phase to extract iodine as I_2. The iodate carrier was reduced carefully with an equivalent amount of Na_2SO_3 in contact with a CCl_4 phase; after separating the phases, more iodate carrier and then Na_2SO_3 were added to the aqueous phase; both fractions were then oxidized with $NaNO_2$ in contact with a CCl_4 phase. The iodine was back-extracted from the three CCl_4 solutions into the aqueous phase with Na_2SO_3. Comparison of the iodine activity in the three fractions was used as an indication of the oxidation state of iodine.

A third procedure incorporated the use of ion exchange resins. For this procedure the original sample was placed on a cation resin column at a pH of 5 to 6. Iodine along with other anions and uncharged particles was washed out with de-ionized water. The wash-through was analyzed for iodine. Procedures for the separation of iodide and iodate on an anion resin column resulted in a good elution of iodide from Dowex 1 resin with 3N-HCl. A number of reagents were tried for an elution of iodate but no satisfactory reagent was found at that time; iodate was not removed by 50 column volumes of 3N-HCl.

3.3.2.2 Results

The results for the analysis of iodine are summarized in Table 3.12. The values showing the distribution of total iodine activity in the solid and liquid phase are accurate to within a few per cent. The growth in and decay of the different isotopes of iodine complicate the procedures and the interpretation of the data. The procedures were not as sensitive nor as satisfactory as those for neptunium to show the presence of the several oxidation states. Furthermore, the oxidation state of iodine in the original fallout probably changed before the samples were recovered. The presence of organic bodies, the susceptability of iodine to air oxidation, possiblities of self-oxidation reduction, and exchange with sea water carrier would contribute to the formation of the resultant oxidation state of iodine in the samples at the time of analysis.

The gamma spectra of the iodine fractions for Shots 2,3, and 4 showed the presence of I^{131}, I^{132}, and I^{133}. The decay of the early sample on Shot 4 indicated a large amount of I^{132} while the gamma spectra showed also the presence of I^{131} and I^{133}.

3.4 COMPOSITION OF THE FALLOUT MATERIAL

The samples analyzed quantitatively consisted of materials collected from the environment of the shot points prior to detonation and the fallout samples. Three coral samples each from sites Charlie and Tare, two surface lagoon sea water samples, one bottom lagoon sea water sample, and one bottom lagoon coral sample were analyzed. Within the limits of variation of the major elements in these samples their chemical analysis was used to determine the amount of environmental or background constituents in the fallout samples. Then, if it is assumed that no great variation in the constituent elements occurred due to fractionation

subsequent to a detonation, the fallout material can be considered as being composed of one or more of the following three components: (1) coral, (2) sea water, and (3) device products (DP). By proper choice of elements, the chemical changes of the constituent compounds of the background components need not be considered. The radioactive device products are treated in other sections.

TABLE 3.12 - Summary of Results for State of Iodine

Shot	Station	Time After Shot	Percentage of Iodine in Solid Phase	Percentage of Total Gamma Count	Apparent Oxidation State
1	250.05,250.06, 251.02	+ 6 to 7 days	50-80	ca 5	-1
2	2-A6	+ 2.5 to + 3.5 days	ca 0	ca 6	-1
3	Coca Head	+ 3 days	93	5	-1
4	airplane wipe	+ 16 hr	ca 0	0.7	-1

3.4.1 Physical Treatment of Samples

The activity of each sample was first measured with a laboratory survey meter. The liquid fraction, if any, was then separated from the solid phase by filtration through a weighed sintered glass frit. The activity of each phase was again measured. The volume and pH of each liquid fraction was then measured and the weight of solid was determined.

In general, the samples treated were portions from the fallout collectors aliquoted at the site laboratory.

3.4.2 Chemical Treatment of Samples

The liquid samples were processed without chemical pre-treatment whenever possible. The solid fractions were dissolved in nitric acid which usually dissolved most of the material. Remaining organic residues were oxidized by the wet ashing method using perchloric acid as the oxidizing agent. Two such perchloric acid treatments usually gave a clear colorless solution. Chemical analysis of the solid fractions was done whenever the total solids were greater than 5 mg.

In general, the chemical treatments of the samples were restricted to a minimum of reagents to prevent as far as possible the addition of elements as impurities which were being determined.

The analytical methods for the various elements are summarized in Tables 3.13 and 3.14. The Beckman flame photometer was specially designed to permit analysis of radioactive samples without hazard to the analysts. The elements Cl, Na, K, Mg, Ca, and Sr were designated as

major constituents; the elements Fe, Al, Cu, Si and Br were designated as minor constituents on the basis of analysis of the background components (coral and lagoon sea water).

TABLE 3.13 - Summary of Analytical Methods

Element	Method(a)	Reagent
Cl	Mohr Titration Method	Silver nitrate
Na	Beckman Flame Photometer	-
K	Beckman Flame Photometer	-
Mg	Beckman Flame Photometer	-
Ca	Beckman Flame Photometer	-
Sr	Beckman Flame Photometer	-
Fe	Beckman Spectrophotometer	Dipyridyl
Al	Beckman Spectrophotometer	Aluminon
Cu	Beckman Spectrophotometer	Diethyldithiocarbamate
Si	Beckman Spectrophotometer	Reduced Silicomolybdate
Br	Beckman Spectrophotometer	Fluorescien-eosin

(a) Application of Analytical Methods to the Analysis of Fallout Material, USNRDL Technical Report in preparation

TABLE 3.14 - Spectrophotometric Analysis of Minor Constituents

Element	Solvent Medium	pH		Wave Length of Max. Absorption (mμ)	Optimum Amount of Sample	
		Permissible Range	Used		Liquid (ml)	Solid (mg)
Fe	H_2O	3.0 - 9.0	5.7	520	>100	10 - 50
Al	H_2O	4.0 - 7.5	4.2	535	10	10 - 25
Cu	CCl_4	5.0 - 9.0 (for extraction)	5.7	435 (in CCl_4)	>100	200-500
Si	H_2O	4.2 - 6.8	4.5-6.0	820 (used 700)	10 - 100	10
Br	H_2O	-	5.7	517	<1	-

The elements Fe, Cu, and Si were characterized by very stable complexes ideally suited for analytical purposes. However, the Si procedure gave soluble Si only. The Al and Br procedures were sensitive to pH and salt concentration. Solutions of Al and Cu could be concentrated without increasing interferences from other elements to any great extent - the Al being carried on $Fe(OH)_3$ and Cu being extracted into CCl_4 as the diethyldithiocarbamate complex.

3.4.3 Results

Analyses of the background components, sea water and coral, are summarized in Table 3.15. The sea water analysis is compared to that given by Sverdrup.[30] The ratio of Cl to the other elements given by Sverdrup was used as the sea water component composition in reducing the data. Ratio values of 1.05×10^{-6} for Fe and 5.3×10^{-7} for Cu were used in the calculations. The coral analyses for sites Charlie and Tare are averages of three samples each of surface coral furnished by Holmes and Narver, Inc. All samples did not give identical analyses; and since they were surface samples, further differences in the ratio of Ca to other elements could have occurred in the fallout coral itself. These analyses, however, were taken as being the best estimate available of the coral component composition.

The physical measurements made on the fallout samples are given in Table 3.16. The fraction of a sampler bottle analyzed was occasionally greater than one when the fallout from more than one bottle was combined. In other cases funnel rinsings were added to the sample so that the fraction is not always the direct ratio of column 1 in Table 3.16 to the total sample as given in Section 3.1.

The concentration analyses of the liquid and solid fractions are given in Tables 3.17 and 3.18. In the cases where the samples were slurries or mixtures of liquid and solid, the comparison of the concentration of the various elements in each phase with those in Table 3.15 for the sea water and coral elements were used to show something about the history of the samples. For example, the consistent high values for 1-250.25 (liquid fraction) indicate evaporation of sea water. This was the case for other samples from Shot 1 where the sample bottles could not be securely sealed, the caps having been destroyed by fire on site Tare.

The concentration analyses of the two fractions were combined for a component analysis of each sample as shown in Table 3.19. The usual procedure was to use the Na and Cl analyses as a basis for the sea water component; when small amounts of Cl were found the Na value was used. After correcting for coral Na, the sea water Na and Cl were recalculated. The ratio values of Table 3.15 were then used to estimate the remaining elements in the sample contributed by sea water. Using the remaining Ca as coral Ca, the ratio values of Table 3.15 for coral were used to estimate the remaining elements as contributed to the fallout from coral. The remainders are attributed as being the contribution of the device-products to the fallout. In most cases positive amounts of Mg remained; this may be due to poor sampling of the background coral (surface coral may not be representative of all the coral thrown up by the detonation). In all cases, excepting one, positive remainders for Fe, Al, and Cu were found. For Shot 1, the island station samples (1-251 series) which contained no liquid were used as a qualitative guide for determining the nature of the fallout. None of these samples show the presence of sea water; the Na remainder after taking out the coral is negative more often than it is positive. The high coral content of many of the island station samples was undoubtedly due to drifting of coral particles into the surface-level pits. The lagoon samples were known to be rinsed together

TABLE 3.15 - Analysis of Background Components

Element	Sea Water (pH = 7.8)			Coral (weight basis)					
	ppm	Ratio		Site Charlie		Site Tare		Lagoon Bottom	
	(mg/l)	NRDL	Sverdrup	(%)	Ratio	(%)	Ratio	(%)	Ratio
Cl	19,570	1	1	0.24	6.7×10^{-3}	0.10	2.8×10^{-3}	-	-
Na	10,610	0.542	0.556	0.31	8.7×10^{-3}	0.31	8.8×10^{-3}	0.69	2.9×10^{-2}
K	390	0.0199	0.0200	0.01	3×10^{-4}	0.01	3×10^{-4}	0.03	1×10^{-3}
Mg	1,313	0.0671	0.0670	2.02	5.68×10^{-2}	3.00	8.46×10^{-2}	0.64	2.7×10^{-2}
Ca	405	0.0207	0.0211	35.6	1	35.4	1	23.7	1
Sr	-	-	6.8×10^{-4}	0.33	9.3×10^{-3}	0.34	9.6×10^{-3}	0.37	1.6×10^{-2}
Fe	< 0.05	$<3\times10^{-6}$	1×10^{-6} - 1×10^{-7}	0.0041	1.1×10^{-4}	0.0043	1.2×10^{-4}	0.0193	3.14×10^{-4}
Al	< 0.01	$<0.5\times10^{-6}$	2.6×10^{-6}	0.00010	2.9×10^{-6}	0.00016	4.6×10^{-6}	0.000058	2.4×10^{-6}
Cu	< 0.08	$<4\times10^{-6}$	5.3×10^{-7} - 5.3×10^{-8}	0.00013	3.5×10^{-6}	0.00018	5.2×10^{-6}	0.00016	6.8×10^{-6}
Si	1.82	9.3×10^{-5}	2×10^{-4} - 1×10^{-6}	0.132	3.7×10^{-3}	0.074	2.1×10^{-3}	0.044	1.9×10^{-3}
Br	-	-	3.4×10^{-3}	-	-	-	-	-	-

TABLE 3.16 - Physical Measurements of the Fallout Samples

Sample	Total Analytical Sample	Fraction of One Sampler Bottle	Wt. Solid[a] Fraction (mg)	Vol. Liquid Fraction (ml)	pH of Liquid Fraction
	(g)				
1-250.04	26.77	1.80	1,204	24.4	11.7
1-250.05	23.39	0.377	394	21.7	7.2
1-250.06	24.12	1.04	398	22.0	7.8
1-250.17	24.36	1.63	34.6	22.0	8.1
1-250.22	4.06	1.41	53.0	3.4	7.6
1-250.24	52.03	1.39	206	49.0	7.5
1-250.25	7.90	2.05	131	6.6	8.1
1-251.02	14.41	0.114	254	14.1	12.0
1-251.03	3.83	0.248	206	3.6	12.2
1-251.04	0.814	0.0250	814	0	-
1-251.05	41.17	0.385	13.9	41.1	7.2
1-251.06	2.78	1.82	2,782	0	-
1-251.07	0.430	0.536	430	0	-
1-251.08	0.608	1.63	608	0	-
1-251.10	0.826	0.549	826	0	-
	(ml)				
2-A4	18.0	0.456	4.1	18.0	7.5
2-A5	5.8	0.126	2.4	5.8	7.9
2-Q4	18.2	0.700	1.8	18.2	-
2-R4	53.6	0.958	5.2	53.6	-
2-T4	9.0	0.300	2.1	9.0	-
3-250.05B[b]	517	0.379	289	517	10.4
3-250.05R[c]	515	0.273	782	515	10.7
3-250.07A	355	0.215	230	355	7.9
3-250.07B	126	0.0764	124	126	8.3
3-250.07C	128	0.120	151	128	8.1
3-251.02	128	0.110	1,033	128	11.5
3-Coca (TC)	128	0.360	326	128	11.9
3-Coca (3C)	128	0.771	45.9	128	7.8
4-Y39	28	1.70	12.5	28	7.4

(a) Density of coral was approximately 2.4

(b) B - Buoy TC

(c) R - Raft TC

TABLE 3.17 - Concentration Analyses of Liquid Fractions from Fallout Samples

Sample	Element (ppm)									
	Cl	Na	K	Mg	Ca	Fe	Al	Cu	Si[a]	Br
1-250.04	15,880	9,000	290	270	1,610	<0.05	0.72	0.67	0.10	59.2
1-250.05	20,450	11,300	385	1,680	660	<0.05	0.69	<0.08	1.43	95.0
1-250.06	25,630	14,800	530	2,350	570	0.07	0.15	0.12	0.94	117
1-250.17	38,640	20,000	845	5.200	796	<0.05	0.58	0.38	1.07	110
1-250.22	62,760	34,000	1,320	6,400	1,740	0.10	0.15	0.025	0.046	-
1-250.24	19,610	10,700	360	1,930	426	<0.05	0.29	0.14	0.59	95.0
1-250.25	60,260	33,500	1,200	6,960	1,340	0.73	0.73	0.38	0.39	-
1-251.02	780	680	31	77	237	0.56	0.43	0.90	0.56	-
1-251.03	1,910	1,348	46	115	284	<0.3	1.48	<0.26	0.30	-
1-251.04	0	0	0	0	0	0	0	0	0	0
1-251.05	920	198	8.0	43	30.8	<0.05	0.27	0.11	1.13	0.80
1-251.06	0	0	0	0	0	0	0	0	0	0
1-251.07	0	0	0	0	0	0	0	0	0	0
1-251.08	0	0	0	0	0	0	0	0	0	0
1-251.10	0	0	0	0	0	0	0	0	0	0
2-A4	2,700	760	34.0	119	38.9	7.98	0.38	3.03	2.50	-
2-A5	5,600	404	16.3	80.8	48.4	3.84	0.76	5.61	0.05	-
2-Q4	-	250	6.7	97.6	26.8	19.8	2.70	7.20	0.10	-
2-R4	-	200	2.5	52.8	19.4	21.5	2.48	2.06	0.10	-
2-T4	-	552	9.2	120	40.4	23.9	4.21	4.26	0.30	-
3-250.05B	142	52.2	2.0	10.6	17.2	<0.05	0.04	<0.08	0.15	-
3-250.05R	100	50.1	2.8	11.6	18.2	0.03	0.04	<0.08	0.18	-
3-250.07a	75.4	50.4	0.8	19.0	18.9	0.01	0.02	<0.08	0.23	-
3-250.07b	83.7	47.2	2.8	6.4	17.2	0.01	0.14	<0.08	0.28	-
3-250.07c	109	25.8	0.8	2.1	12.2	<0.05	0.10	<0.08	1.03	-
3-251.02	58.6	16.1	3.0	9.5	20.5	<0.05	0.06	<0.08	0.43	-
3-Coca (TC)	259	120	6.6	8.5	41.6	0.16	<0.06	<0.08	7.72	-
3-Coca (3C)	276	34.0	2.6	8.5	111	<0.05	0.19	<0.08	0.23	-
4-Y39	21,130	12,620	374	1,690	412	1.88	0.27	0.27	0.74	21.0

(a) As soluble silica

TABLE 3.18 - Concentration Analyses of Solid Fractions from Fallout Samples

Sample	Element (Wt. %)								
	Na	K	Mg	Ca	Sr	Fe	Al	Cu	Si[a]
1-250.04	0.509	0.020	3.79	38.1	0.50	0.0282	0.0121	<0.0034	0.0009
1-250.05	0.990	0.050	9.82	28.6	0.45	0.0147	0.0234	<0.0037	0.0069
1-250.06	0.980	0.039	7.74	34.7	0.40	0.0250	0.0143	<0.0037	0.0011
1-250.17	3.80	0.18	4.34	19.9	-	0.0872	0.0737	0.0268	0.0157
1-250.22	12.1	0.34	1.42	15.1	0.034	0.171	0.116	0.0131	0.0051
1-250.24	0.396	0.019	7.44	36.5	0.32	0.0667	0.0125	0.0189	0.0003
1-250.25	1.00	0.036	5.87	33.5	0.18	0.0910	0.0213	0.0285	0.0007
1-251.02	0.239	0.013	2.62	43.6	0.47	0.0338	0.0139	0.0078	0.0014
1-251.03	0.181	0.0028	2.33	44.0	0.41	0.0433	0.0142	<0.0036	0.0019
1-251.04	0.102	0.0073	2.31	37.4	0.46	0.0044	0.0354	0.0022	0.0024
1-251.05	0.105	0.0	1.27	24.4	-	0.0834	0.0176	0.0192	0.0211
1-251.06	0.243	0.0090	2.78	38.9	0.54	0.0200	0.0444	0.0021	0.0150
1-251.07	0.258	0.0075	2.26	37.7	0.62	0.0617	0.0097	0.0057	0.0002
1-251.08	0.372	0.024	2.62	37.7	0.50	0.0095	0.0062	<0.0034	0.0006
1-251.10	0.263	0.0089	2.08	36.9	0.72	0.0223	0.0112	0.0153	0.0006
2-A4	-	-	-	-	-	-	-	-	-
2-A5	-	-	-	-	-	-	-	-	-
2-Q4	-	-	-	-	-	-	-	-	-
2-R4	-	-	-	-	-	-	-	-	-
2-T4	-	-	-	-	-	-	-	-	-
3-250.05B	0.134	0.006	4.06	38.1	0.36	0.180	0.0494	0.0266	<0.0011
3-250.05R	0.154	0.006	3.23	37.0	0.43	0.099	0.0134	0.0042	0.0046
3-250.07a	0.164	0.025	2.90	35.1	0.47	0.336	0.0418	0.0086	<0.0012
3-250.07b	0.171	0.038	0.80	35.5	0.39	0.189	0.0254	0.0089	0.00025
3-250.07c	0.203	0.008	2.29	39.1	0.42	0.687	0.0105	<0.0089	0.00075
3-251.02	0.205	0.008	2.99	35.6	0.31	0.0309	0.00726	0.0080	<0.0010
3-Coca (TC)	0.170	0.003	3.84	36.5	0.36	0.403	0.0199	0.0224	0.00038
3-Coca (3C)	0.159	0.007	2.04	28.3	0.037	0.959	1.29	0.0477	0.00074
4-Y39	20.6	0.662	2.89	2.46	-	1.05	0.194	0.0719	<0.020

(a) As soluble silica

TABLE 3.19 - Component Analysis of Fallout Samples

Sample	Component	Element (mg)									
		Cl	Na	K	Mg	Ca	Sr	Fe	Al	Cu	
1-250.04	Total	388	226	7.24	52.2	498	6.0	0.339	0.164	0.016	<0.057
	Sea Water	393	219	7.86	26.3	8	.3	0.0004	0.001	0.0002	
	Coral	3	4	0.14	27.8	490	4.5	0.056	0.001	0.0017	
	D.P.(a)	-8	+3	-0.76	-1.9	0	+1.2	+0.283	+0.162	0.014	<0.055
1-250.05	Total	444	249	8.55	75.2	127	1.8	0.0580	0.107	<0.017	
	Sea Water	445	247	8.90	29.8	9	0.3	0.0005	0.001	0.0002	
	Coral	1	1	0.03	6.7	118	1.1	0.0134	0.0003	0.0004	
	D.P.	-2	+1	-0.38	+38.7	0	+0.4	+0.0241	+0.106	<0.016	
1-250.06	Total	564	330	11.8	82.5	151	1.6	0.101	0.0602	0.0026	<0.0176
	Sea Water	577	321	11.5	38.6	12	0.4	0.0006	0.0015	0.0003	
	Coral	1	1	0.04	7.9	139	1.2	0.0158	0.0004	0.0005	
	D.P.	-14	+8	+0.3	+36.0	0	0	+0.085	+0.0583	0.0018	<0.0168
1-250.17	Total	850	441	18.6	116	24.4	-	0.0302	0.0383	0.101	
	Sea Water	822	457	16.4	55	17.3	0.6	0.0009	0.0022	0.0004	
	Coral	0.05	0.06	0.002	0.4	7.1	0.07	0.0008	0.00002	0.00002	
	D.P.	+28	-16	+2.2	+61	0	-	+0.0285	+0.0361	+0.101	
1-250.22	Total	213	122	4.67	22.5	13.9	0.016	0.0909	0.0621	0.00702	
	Sea Water	216	120	4.33	14.5	4.5	0.15	0.0002	0.0006	0.00011	
	Coral	0.1	0.1	0.003	0.5	9.4	0.09	0.0011	0.00003	0.00003	
	D.P.	-3	+2	+0.34	+7.5	0	-0.22	+0.0896	+0.0615	+0.00688	
1-250.24	Total	961	525	17.7	110	96.0	0.66	0.137	0.0399	0.0458	
	Sea Water	952	529	19.0	64	20.0	0.65	0.001	0.0025	0.0005	
	Coral	0.5	0.7	0.02	4	76.0	0.004	0.009	0.0002	0.0003	
	D.P.	+9	-5	-1.3	+42	0	+0.01	+0.127	+0.0372	+0.0450	
1-250.25	Total	398	222	7.97	53.6	52.8	0.24	0.0167	0.0327	0.0399	
	Sea Water	398	222	7.97	26.7	8.4	0.27	0.0004	0.0010	0.0002	
	Coral	0.3	0.4	0.01	2.5	44.4	0.41	0.0051	0.0001	0.0002	
	D.P.	0	0	-0.01	+24.4	0	-0.44	+0.0112	+0.0316	+0.0395	

TABLE 3.19 - Component Analysis of Fallout Samples (Continued)

Sample	Component	Element (mg)								
		Cl	Na	K	Mg	Ca	Sr	Fe	Al	Cu
1-251.02	Total	11.0	10.2	0.47	7.7	114	1.2	0.0936	0.0412	0.0324
	Sea Water	16.6	9.2	0.33	1.1	0.3	0.01	0.00002	0.00004	0.000009
	Coral	0.8	1.0	0.03	6.4	114	1.2	0.0130	0.0004	0.0004
	D.P.	-6.4	0	+0.11	+ 0.2	0	0	+ 0.0806	+ 0.0408	+0.0320
1-251.03	Total	6.89	5.22	0.17	5.20	91.5	0.84	0.0898	0.0345	<0.0168
	Sea Water	7.96	4.43	0.16	0.53	0.2	0.005	0.000008	0.00002	0.000004
	Coral	0.62	0.79	0.03	5.18	91.3	0.84	0.0104	0.0003	0.0003
	D.P.	-1.69	0	-0.02	-0.51	0	0	+ 0.0794	+ 0.0342	<0.0165
1-251.04	Total	-	0.83	0.059	18.8	304	3.7	0.0357	0.118	0.0181
	Coral	-	2.65	0.086	17.3	304	2.8	0.0347	0.0009	0.0011
	D.P.	-	-1.82	-0.027	+1.5	0	+ 0.9	+ 0.0010	+ 0.117	+0.0170
1-251.05	Total	37.8	8.15	0.33	1.96	4.66	-	0.0116	0.0135	0.00719
	Sea Water	14.6	8.11	0.29	0.98	0.31	0.01	0.00002	0.00004	0.000008
	Coral	0.03	0.04	0.001	0.25	4.35	0.04	0.0005	0.00001	0.00002
	D.P.	+ 23.3	0	+0.04	+ 0.73	0	-	+ 0.0111	+ 0.0135	+0.00716
1-251.06	Total	-	6.76	0.25	77.3	1,080	15	0.0557	0.373	0.0175
	Coral	-	9.43	0.30	61.4	1,080	10	0.1234	0.003	0.0038
	D.P.	-	-2.67	-0.05	+15.9	0	+ 5	-0.0677	+ 0.370	+0.0137
1-251.07	Total	-	1.11	0.032	9.71	162	2.7	0.0265	0.0416	0.0244
	Coral	-	1.41	0.045	9.18	162	1.5	0.0184	0.0005	0.0006
	D.P.	-	-0.30	-0.013	+ 0.53	0	+1.2	+ 0.0081	+ 0.0411	+0.0238
1-251.08	Total	-	2.26	0.15	15.9	229	3.0	0.0578	0.0376	<0.021
	Coral	-	2.00	0.06	13.0	229	2.1	0.0262	0.0007	0.0008
	D.P.	-	+ 0.26	+0.09	+ 2.9	0	+ 0.9	+ 0.0316	+ 0.0369	<0.020
1-251.10	Total	-	2.17	0.074	17.2	305	5.9	0.184	0.0924	0.0126
	Coral	-	2.66	0.086	17.3	305	2.8	0.035	0.0009	0.001
	D.P.	-	-0.49	-0.012	-0.1	-	+ 3.1	+ 0.149	+ 0.0915	+0.125

TABLE 3.19 - Component Analysis of Fallout Samples (Continued)

Sample	Component	Element (mg)								
		Cl	Na	K	Mg	Ca	Sr	Fe	Al	Cu
2-A4	Total	49	13.7	0.61	2.14	0.700	-	0.144	0.0068	0.0545
	Sea Water	25	13.7	0.49	1.65	0.518	-	0.00003	0.00006	0.000001
	Coral	0.001	0.001	0.00005	0.001	0.182	-	0.00002	-	-
	D.P.	+24	0	+0.12	+0.49	0	-	+0.144	+0.0067	+0.0545
2-A5	Total	32	2.34	0.094	0.469	0.281	-	0.0208	0.0043	0.0326
	Sea Water	4.2	2.34	0.084	0.282	0.089	-	0.000005	0.00001	0.000002
	Coral	0.001	0.002	0.00005	0.001	0.192	-	0.00002	-	-
	D.P.	+28	0	+0.010	+0.186	0	-	+0.0208	+0.0043	+0.0326
2-Q4	Total	-	4.55	0.12	1.78	0.488	-	0.360	0.0491	0.131
	Sea Water	-	4.55	0.16	0.55	0.172	-	0.000009	0.00002	0.000004
	Coral	-	0.003	0.00009	0.002	0.316	-	0.00004	-	-
	D.P.	-	0	-0.04	+1.23	-	-	+0.360	+0.0491	+0.131
2-P4	Total	-	10.7	0.13	2.83	1.04	-	1.15	0.133	0.110
	Sea Water	-	10.7	0.38	1.29	0.40	-	0.00002	0.00005	0.00001
	Coral	-	0.006	0.0002	0.004	0.64	-	0.00007	-	-
	D.P.	-	0	-0.25	+1.54	0	-	+1.15	+0.133	+0.110
2-T4	Total	-	4.97	0.083	1.08	0.364	-	0.215	0.0379	0.0383
	Sea Water	-	4.97	0.179	0.60	0.188	-	0.00009	0.0002	0.000005
	Coral	-	0.002	0.00005	0.001	0.176	-	0.00002	-	-
	D.P.	-	0	-0.096	+0.48	0	-	+0.215	+0.0377	+0.0383
3-250.05B	Total	73.4	27.4	1.0	17.2	119	1.0	0.521	0.164	0.077	< 0.118
	Sea Water	47.4	26.4	0.9	3.2	1	0.03	0.00005	0.00001	0.00002	
	Coral	0.3	1.0	0.03	10.0	118	1.0	0.014	0.0005	0.0006	
	D.P.	+25.7	0	+0.1	+4.0	0	0	+0.507	+0.164	0.076	< 0.117
3-250.05R	Total	51.5	27.0	1.5	31.2	299	3.4	0.789	0.125	0.033	< 0.074
	Sea Water	43.8	24.4	0.9	2.9	1	0.03	0.00004	0.0001	0.00002	
	Coral	0.8	2.6	0.08	25.2	298	2.9	0.036	0.0014	0.002	
	D.P.	+ 6.9	0	+0.5	+3.1	0	+0.5	+0.753	+0.124	0.031	< 0.072

TABLE 3.19 - Component Analysis of Fallout Samples (Concluded)

Sample	Component	Element (mg)									
		Cl	Na	K	Mg	Ca	Sr	Fe	Al	Cu	
3-250.07a	Total	26.8	18.3	0.34	13.4	87.4	1.1	0.776	0.0968	0.20	<0.048
	Sea Water	31.4	17.5	0.63	2.1	0.7	0.02	0.00003	0.00008	0.00002	
	Coral	0.3	0.8	0.02	7.3	86.7	0.8	0.011	0.0004	0.0004	
	D.P.	-4.9	0	-0.31	+4.0	0	+0.2	+0.765	+0.0963	0.020	<0.048
3-250.07b	Total	10.5	6.16	0.40	1.80	46.1	0.48	0.234	0.0490	0.011	<0.021
	Sea Water	10.4	5.76	0.21	0.69	0.2	0.007	0.00001	0.00003	0.000006	
	Coral	0.1	0.40	0.01	3.88	45.9	0.44	0.006	0.0002	0.0002	
	D.P.	0	0	+0.18	-2.77	0	+0.03	+0.228	+0.0488	0.011	<0.021
3-250.07c	Total	14.0	3.61	0.11	3.73	60.6	0.63	1.04	0.0287	<0.0235	
	Sea Water	5.5	3.08	0.11	0.37	0.1	0.003	0.000005	0.00002	0.000003	
	Coral	0.2	0.53	0.017	5.12	60.5	0.58	0.007	0.0003	0.0003	
	D.P.	+8.3	0	0	-1.46	0	+0.05	+1.03	+0.0284	<0.0232	
3-251.02	Total	7.50	4.18	0.47	32.1	391	3.2	0.319	0.0827	0.083	<0.093
	Sea Water	1.35	0.75	0.03	0.1	0.03	0.001	0.000001	0.000004	0.0000007	
	Coral	1.10	3.43	0.11	33.1	391	3.8	0.048	0.0018	0.002	
	D.P.	+5.05	0	+0.33	-1.1	0	-0.6	+0.271	+0.0809	0.081	<0.091
3-Coca TC	Total	33.1	15.9	0.86	13.5	124	1.2	1.33	0.0649	0.073	<0.083
	Sea Water	26.6	14.8	0.53	1.8	0.6	0.02	0.00003	0.00007	0.00001	
	Coral	0.4	1.1	0.04	10.5	123	1.2	0.02	0.0006	0.0006	
	D.P.	+6.1	0	+0.29	+1.2	123	0	+1.31	+0.0642	0.072	<0.083
3-Coca 3C	Total	35.3	4.42	0.34	2.02	27.2	0.18	0.443	0.617	0.022	<0.032
	Sea Water	7.5	4.19	0.15	0.50	0.2	0.005	0.000008	0.00002	0.000004	
	Coral	0.1	0.24	0.008	2.29	27.0	0.26	0.003	0.0001	0.0001	
	D.P.	+27.7	0	+0.20	-0.77	0	-0.08	+0.440	+0.617	0.022	<0.032
4-T39	Total	592	353	10.6	47.7	11.6	-	0.184	0.0318	0.0166	
	Sea Water	613	341	12.3	41.1	12.9	-	0.0006	0.0016	0.0003	
	D.P.	-21	+12	-1.7	+6.6	-1.3	-	+0.183	+0.0302	+0.0163	
	Sea Water[b]	93.2	51.8	1.9	6.2	2.0					

(a) Device Product

(b) 15.2% of total sea water elements as fallout material

with the aid of lagoon sea water. Although the analyses for a number of these samples indicated various stages of evaporation, the amount of the various sea water constituents was generally in the correct order. On the other hand, the sea water rinsing of two bottles into the third provided samples in which the recovery of the total fallout was far greater than when the dry material was collected without rinsing. For this reason, the amounts of fallout material as coral or device-products from the lagoon stations (1-250 series) were considered the most valid. Hence, the fallout material from Shot 1 consisted of coral and the device-product components. The material from Shot 2 showed the presence of all three components. Three of the samples were combined acid (HCl) washes of funnel and bottle so the Cl analysis was not included. Small amounts of residue (carbonaceous) were not analyzed. The fallout from Shot 3 also contained significant amounts of all three components in addition to large volumes of rain water. The rain washed down the funnels. Only one sample from Shot 4 was analyzed; the analysis of this sample gave a 15.2 per cent excess concentration (based on Cl, Na, and Mg analysis) of sea water but no remainder as coral; however, the sample was known to have been exposed too short a time for evaporation of that extent to occur so that the excess was attributed to fallout.

The field teams of Project 2.5a inspected the collectors periodically to remove extraneous material from the bottle collectors; however, it was not always possible to make such an inspection immediately prior to shot time at all stations. Therefore, when analyses indicate, the island station samples may be assumed to be high in coral while the raft or buoy (or YAG) station collectors high in sea water constituents. For any shot, the best estimate of the amount of coral would accordingly be obtained from a collector stationed in the lagoon while the best estimate of the amount of sea water in the fallout would be obtained from a sampler stationed on an island. Any departure of sea water constituents from the lagoon water concentration would indicate either evaporation or collection of rain water. Samplers mounted on buoys were further from the water than those mounted on rafts; hence the amount of spray collected by buoy samplers would be less than that collected by raft samplers and should give a better estimate of sea water in the fallout as well as a better estimate for the radioactive material. These considerations, along with those given in the preceding paragraph, are used in the following discussion of the data.

The surface density of the three components, coral, sea water, and device products are tabulated in Table 3.20. The density distributions are plotted in Figs. 3.12 through 3.14. The surface densities are calculated for the 7-in. diameter funnel in terms of the original (unchanged) component material. Due to limitations of time and manpower as well as considerations of application of the data, analyses to determine the amounts of pyrolyzed and non-pyrolyzed coral were not attempted. If they had been, estimates of extraneous material (as drift-in) might have been made. From appearances of the samples, however, the coral component from Shots 1 and 2 was essentially all pyrolyzed coral while that from Shot 3 appeared to contain large amounts of unchanged coral.

The surface density of equivalent coral on Shot 1 ranged from about 50 to 3000 mg/sq ft for the lagoon station samples. On Shot 2 (buoy

TABLE 3.20 - Surface Density of Fallcut Components

Sample	Coral		Sea Water		Device	
	Total Ca (mg)	Density[a] (mg/sq ft)	Total Na (mg)	Density[b] (ml/sq ft)	Total Fe (mg)	Density[c] (fraction/sq ft) x 10^{12}
1-250.04	272	2,860	0	0	0.157	10.6[d]
1-250.05	313	3,290	0	0	0.064	4.30
1-250.06	134	1,410	0	0	0.082	5.50
1-250.17	4.4	46	0	0	0.018	1.20
1-250.22	6.7	70	0	0	0.064	4.30
1-250.24	55	580	0	0	0.091	6.12
1-250.25	22	230	0	0	0.0055	0.37
1-251.02	1,000	10,700	0	0	0.707	4.76
1-251.03	368	3,870	0	0	0.320	21.5
1-251.04	12,200	128,000	0	0	0.040	2.69
1-251.05	11	120	0	0	0.029	1.95
1-251.06	594	6,240	0	0	-	-
1-251.07	302	3,170	0	0	0.015	1.01
1-251.08	140	1,470	0	0	0.019	1.28
1-251.10	556	5,840	0	0	0.272	18.3
2-A4	0.40	4.2	30.0	10.6	0.315	5.01
2-A5	1.52	16.0	18.6	6.56	0.165	2.62
2-Q4	0.45	4.7	6.5	2.29	0.514	8.18
2-R4	0.67	7.0	11.2	3.95	1.20	19.1
2-T4	0.59	6.2	16.6	5.86	0.717	11.4
3-250.05B	312	3,300	69.7	24.6	1.34	98.2
3-250.05R	1,090	11,500	89.4	31.5	2.76	202
3-250.07a	403	4,260	81.4	28.7	3.56	261
3-250.07b	601	6,350	75.4	26.6	2.98	218
3-250.07c	504	5,320	25.7	9.06	8.59	629
3-251.02	3,550	37,500	6.82	2.40	2.46	180
3-Coca TC	342	3,610	41.1	14.5	3.64	267
3-Coca 3C	35	370	5.44	1.92	0.570	41.7
4-Y39	0	0	30.5	10.8	0.108	1.52

(a) In terms of original coral composition (b) In terms of original sea water composition

(c) From total steel in device and device-site construction

(d) Values for Shot 1 for above grade materials only

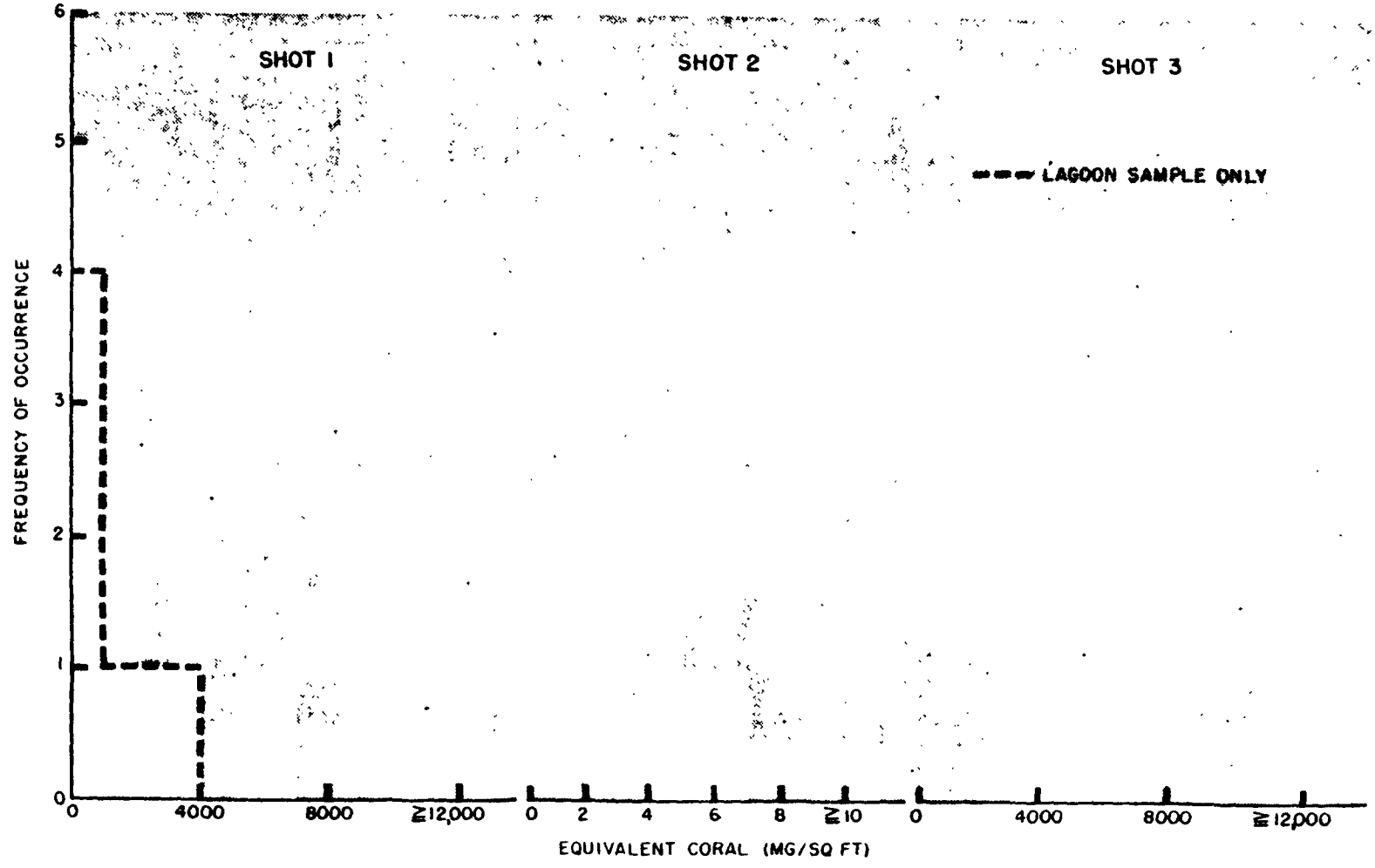

Fig. 3.12 Density Distribution of Equivalent Coral for Shots 1,2, and 3

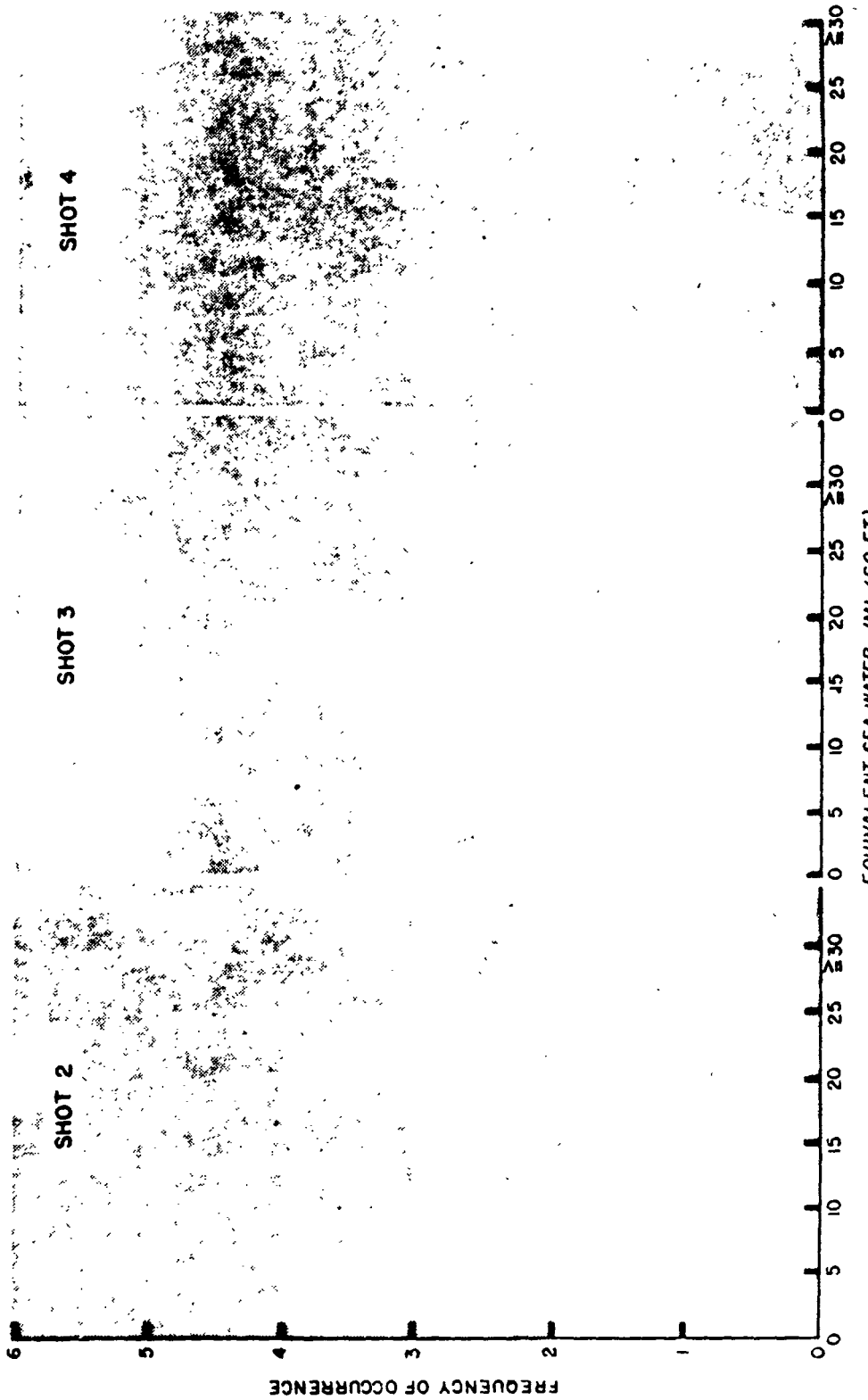

Fig. 3.13 Density Distribution of Equivalent Sea Water for Shots 2,3, and 4

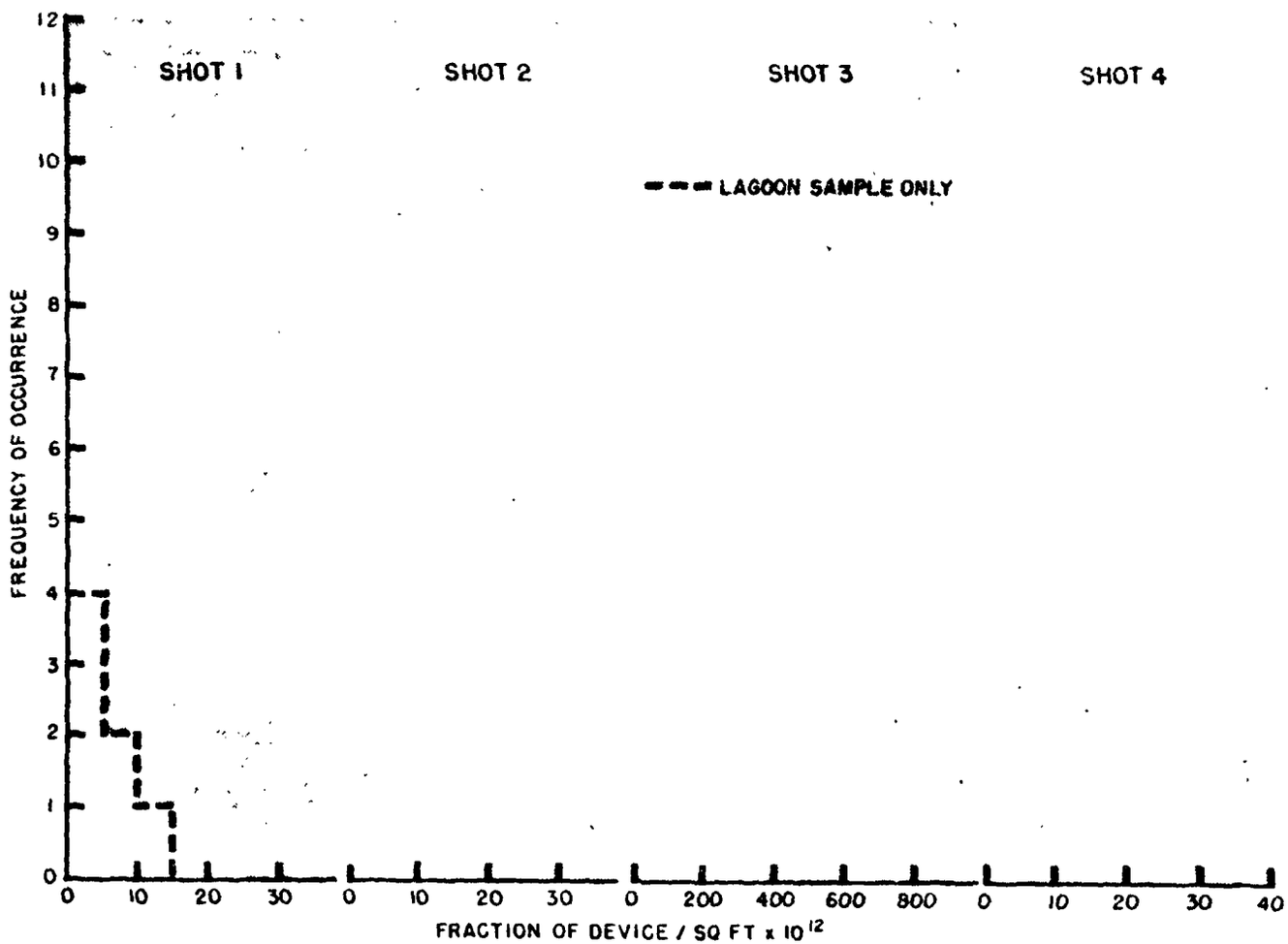

Fig. 3.14 Density Distribution of Device Fraction for Shots 1,2,3, and 4

samples), the surface density ranged from 4 to 7 mg/sq ft (with one sample at 16). On Shot 3, the surface density of coral ranged from 3000 to 7000 mg/sq ft (with one sample at 12,000).

The surface density of equivalent sea water on Shot 2 ranged from 2 to 11 ml/sq ft. The samples collected were both dry and wet. For those containing liquid, the concentration analyses gave too low values to indicate a pure sea water splash-in. Some rain was experienced during recovery of these samples. Hence, Shot 2 fallout was probably essentially a dry material when it arrived at the collectors. On Shot 3, the surface density of sea water ranged from 2 to 30 ml/sq ft. The island station and 3-bottle sampler values were near the lower end of the range; the total collector on Coca Head gave a mid-range value; the total collectors on the lagoon rafts and buoys generally gave values at the high end of the range as shown by the split distribution plot. No definite information is available as to when the sample bottles were last checked for splash-in prior to shot time. It seems likely, however, from the analyses alone that the higher distribution was due to splash-in and that the 2 to 15 ml/sq ft surface density is the more reliable distribution. On Shot 4, the single sample gave a value of 11 ml/sq ft for the equivalent surface density of the sea water component.

The surface density of the device is given for Fe in terms of fraction of the device which fell on each square foot range from about 1×10^{-12} to 10×10^{-12} on Shot 1 for the lagoon station samples. A mid-range fractional density of 4.3×10^{-12} per sq ft would give (as a minimum) a coverage of about 8000 sq mi for a 100 per cent fallout. On Shot 2, the fractional surface density for the device ranged from about 3×10^{-12} to 20×10^{-12} per sq ft. On Shot 3, the fractional surface density ranged from about 100×10^{-12} to 300×10^{-12} for the majority of samples. A mid-range fractional density of 230×10^{-12} per sq ft would give a coverage of about 160 sq mi for a 100 per cent fallout. The areas for a 100 per cent fallout are given only for a qualitative check on the analytical data and do not indicate the actual coverage such as do the fallout distributions as given in the CASTLE report of Project 2.5a. If it would have been possible to analyze the fallout samples at more stations, fallout contours of surface density of coral, sea water, and device products could have been determined for comparison with the dosage contours. On Shot 4, the one value at 1.5×10^{-12} per sq ft was about a factor of 3 less than the mid-range value for Shot 1 and roughly a factor of 5 or 6 less than that for Shot 2.

A comparison of an estimated radiation field to the surface density of each component is made in Table 3.21, with the corresponding distributions given by Figs. 3.15 through 3.17. The total gamma counts for each fallout collector bottle (taken in the same geometry) were corrected back to 1 hr from a calculated beta decay scheme (see Chapter 5). For Shot 1, the estimated radiation field reading at 1 hr given by Project 2.5a was used. On Shots 2 and 4, preliminary estimates of the field were made using uncorrected data taken from recorded data on a 50 x 50 ft section of flight deck of the YAG 40 at as early a time as possible (5 to 16 hr). These readings were compared to the total gamma count in the Project 2.5a total collectors. On Shot 2, the ratio of r/hr to c/m ranged from 0.026×10^{-7} to 0.051×10^{-7} while on Shot 4, the ratio

TABLE 3.21 - Comparison of Radiation Field with Surface Density of Fallout Components

Sample	Total Gamma Count per bottle (c/m x 10^{-7} at 1 hr)	Estimated Equivalent Field (r/hr at 1 hr)	Ratio of Field to Coral Surface Density (r/hr:mg/sq ft)	Ratio of Field to Sea Water Surface Density (r/hr:ml/sq ft)	Ratio of Field to Device Fractional Density (r/hr:fraction/sq ft) x 10^{-12}
1-250.04	2,400	100(a)	0.035	0	9
1-250.05	4,800	80(a)	0.024	0	19
1-250.06	1,500	80(a)	0.057	0	15
1-250.17	15	50(a)	1	0	25
1-250.22	150	26(a)	0.4	0	6
1-250.24	2,100	28(a)	0.048	0	5
1-250.25	50	30(a)	0.13	0	80
1-251.02	89,000	1,650(a)	0.15	0	350
1-251.03	11,000	600(a)	0.15	0	28
1-251.04	6,900	350(a)	0.003	0	130
1-251.05	200	210(a)	1.7	0	110
1-251.06	2,900	60(a)	0.01	0	-
1-251.07	10	22(a)	0.007	0	22
1-251.08	-	19(a)	0.01	0	15
1-251.10	20	30(a)	0.005	0	2
2-A4	2,200	120	29	11	24
2-A5	1,700	90	6	14	34
2-O4	40	2	-	-	-
2-P4	2	0.1	-	-	-
2-Q4	2,000	110	23	48	13
2-R4	9,000	480	69	120	25
2-T4	1,700	90	15	15	?
2-Y39	310	20	-	-	-
2-Y40	2,600	140(b)	-	-	-
3-250.05B	8,300	440	0.14	18	4.5
3-250.05R	8,500	450	0.039	14	2.2
3-250.07a	4,500	240	0.056	8	0.9
3-250.07b	4,500	240	0.038	9	1.1

TABLE 3.21 - Comparison of Radiation Field with Surface Density of Fallout Components (Concluded)

Sample	Total Gamma Count per bottle (c/m x 10^{-7} at 1 hr)	Estimated Equivalent Field (r/hr at 1 hr)	Ratio of Field to Coral Surface Density (r/hr:mg/sq ft)	Ratio of Field to Sea Water Surface Density (r/hr:ml/sq ft)	Ratio of Field to Device Fractional Density (r/hr:fraction/sq ft x 10^{-12})
3-250.07c	7,100	380	0.071	42	0.6
3-251.02	9,900	520	0.014	220	2.9
3-Coca TC	14,400	770	0.21	53	2.9
3-Coca 3C	900	50	0.14	26	1.2
3-250.08	9,600	510	-	-	-
4-Y39	2,300	120	0	11	79
4-Y40P	660	40	-	-	-
4-Y40S	2,000	110(b)	-	-	-

(a) Average of Rad Safe and/or Project 2.5a surveys (see Project 2.5a report)

(b) Estimate from Project 6.4 preliminary uncorrected data (see text)

TABLE 3.21 - Comparison of Radiation Field with Surface Density of Fallout Components (Concluded)

Sample	Total Gamma Count per bottle (c/m x 10^{-7} at 1 hr)	Estimated Equivalent Field (r/hr at 1 hr)	Ratio of Field to Coral Surface Density (r/hr:mg/sq ft)	Ratio of Field to Sea Water Surface Density (r/hr:ml/sq ft)	Ratio of Field to Device Fractional Density (r/hr:fraction/sq ft x 10^{-12})
3-250.07c	7,100	380	0.071	42	0.6
3-251.02	9,900	520	0.014	220	2.9
3-Coca TC	14,400	770	0.21	53	2.9
3-Coca 3C	900	50	0.14	26	1.2
3-250.08	9,600	510	-	-	-
4-Y39	2,300	120	0	11	79
4-Y40P	660	40	-	-	-
4-Y40S	2,000	110(b)	-	-	-

(a) Average of Rad Safe and/or Project 2.5a surveys (see Project 2.5a report)

(b) Estimate from Project 6.4 preliminary uncorrected data (see text)

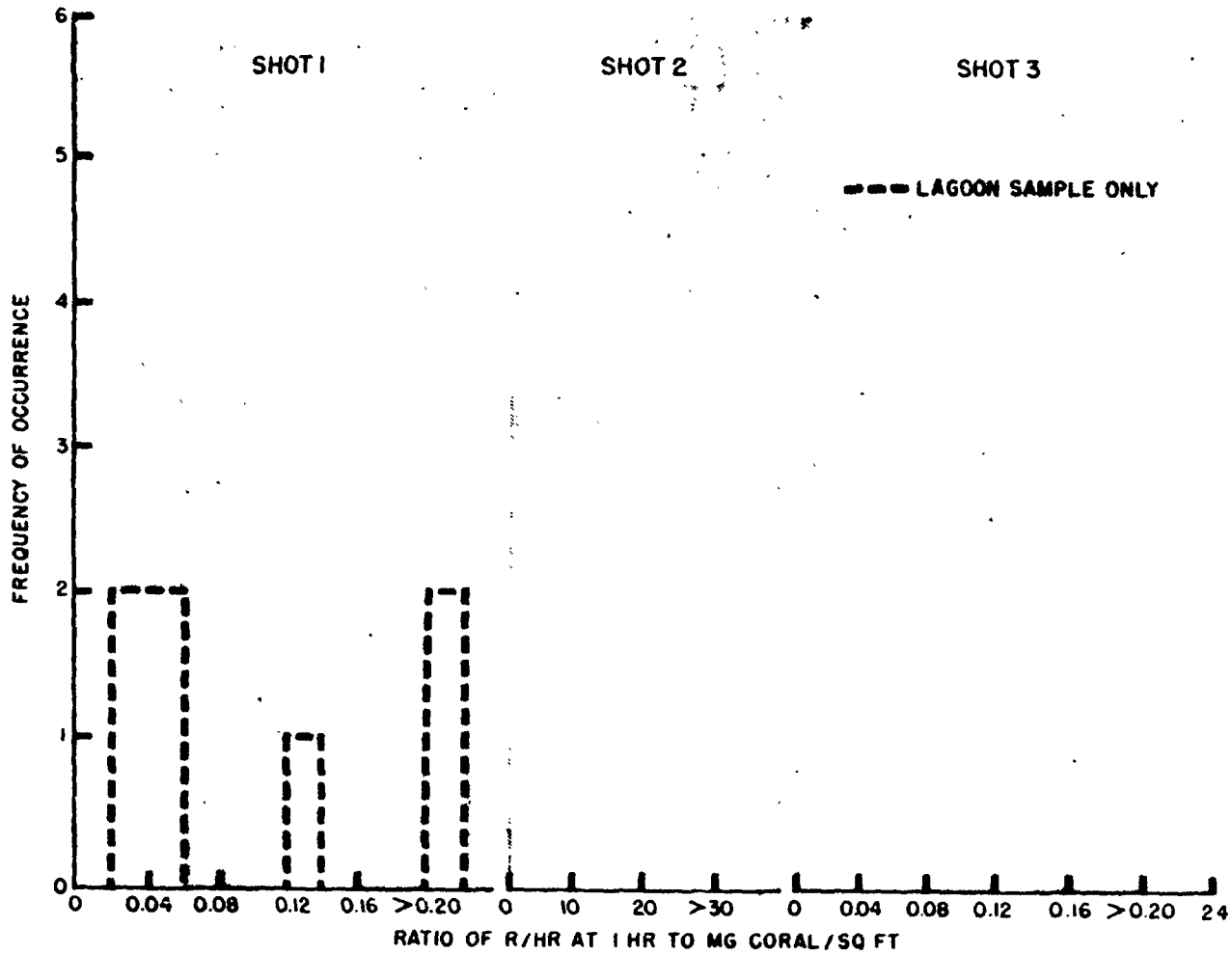

Fig. 3.15 Distribution of the Ratio of the Radiation Field to the Surface Density of the Coral Component

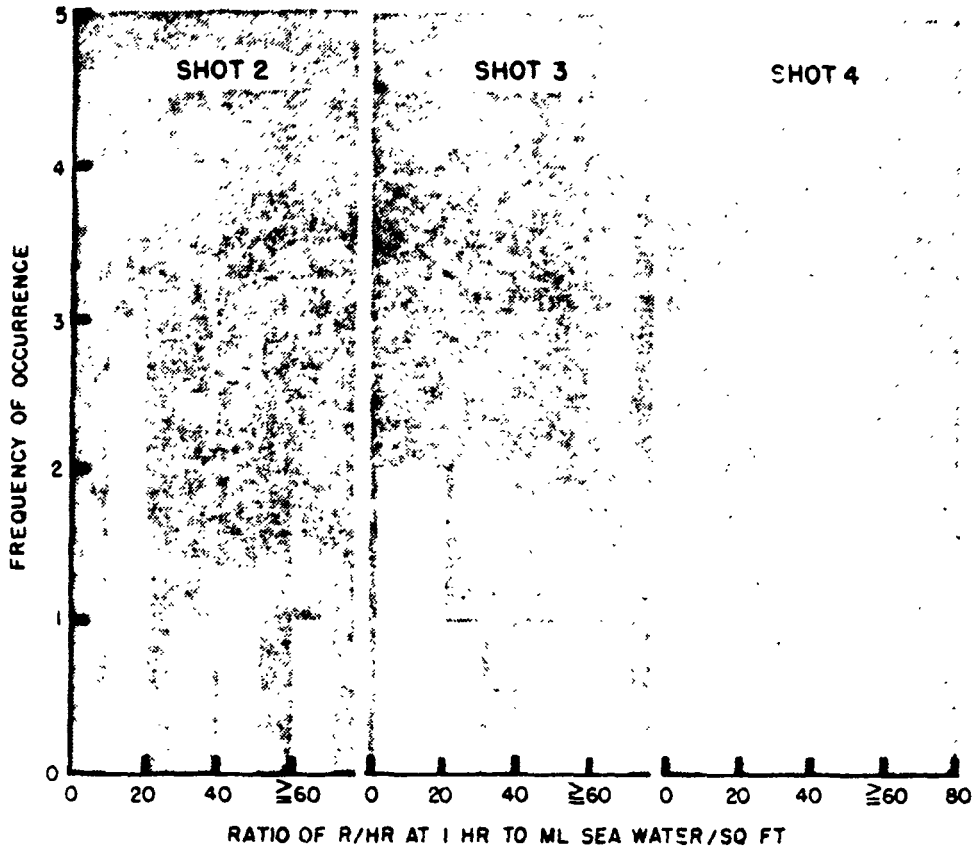

Fig. 3.16 Distribution of the Ratio of the Radiation Field to the Surface Density of the Sea Water Component

varied from 0.045×10^{-7} to 0.070×10^{-7}. For samples 251.03 and 251.04 on Shot 1, using only the island survey data (as corrected to 1 hr by Project 2.5a) gave a ratio of 0.045×10^{-7} to 0.064×10^{-7} and 0.043×10^{-7} to 0.058×10^{-7} while other island station samples gave ratios varying from 0.01×10^{-7} to 1.0×10^{-7} when similarly compared. Excepting for those noted in Table 3.21, a factor 0.053×10^{-7} was used to estimate the field reading from the total gamma count. If the assumption of complete mixing of the three components with the radioactive device components is valid and if the sampling techniques are sound so that the sample is a representation of the over-all fallout in the particular area, then the ratio of the field radiation to the surface density of the tracer fallout components should be a constant for each shot. The comparisons as given in Table 3.21 show large variations instead of constancy. Actual field readings were available only for Shot 1 island stations where the sample recovery was actually the most questionable. The extent of error in the

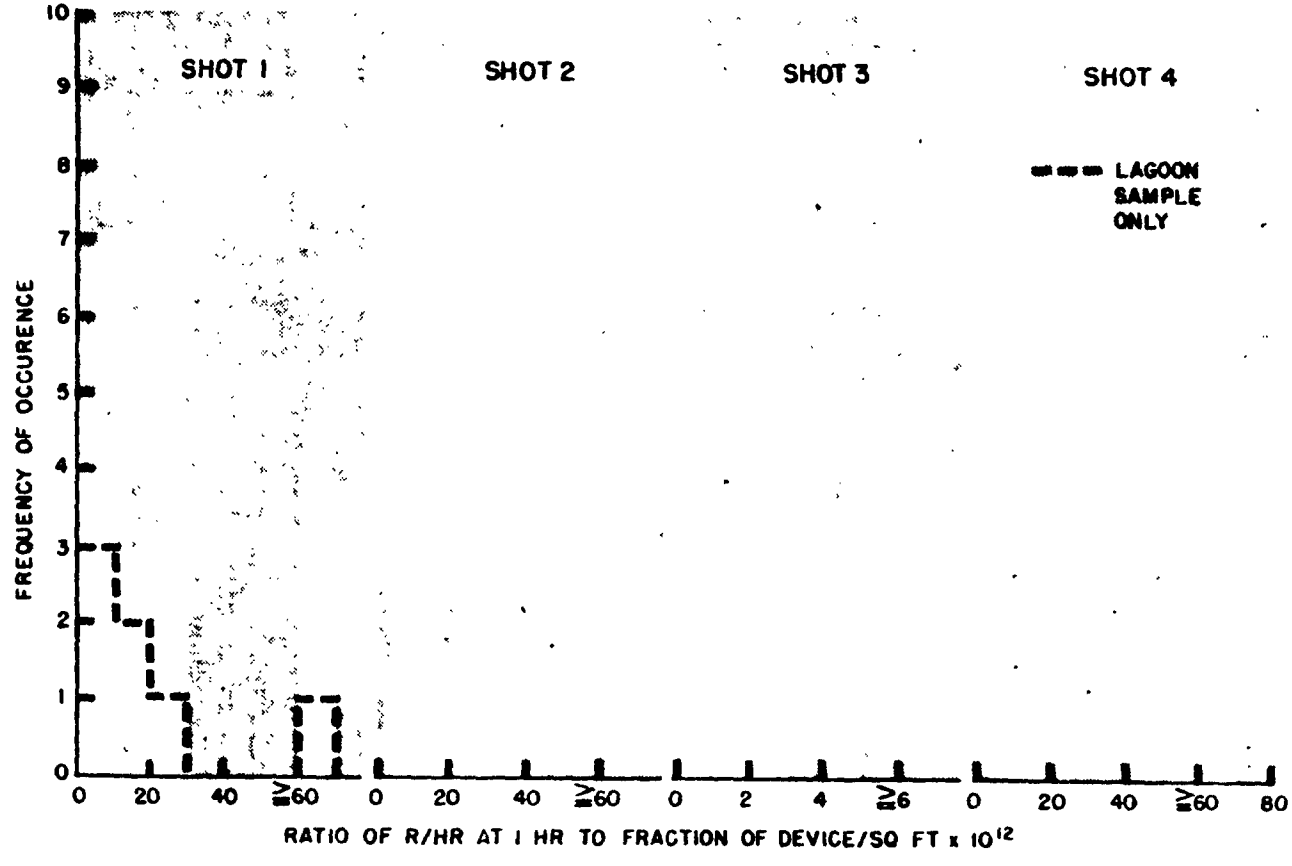

Fig. 3.17 Distribution of the Ratio of the Radiation Field to the Surface Density of the Device Fraction Component

given field reading corresponding to the sample area for all other samples is entirely unknown. With the available data and in view of the sample treatment from recovery to analysis, the following values were selected as a set of reasonable values for the radiation field to surface density ratio: (1) Coral (ratio of r/hr at 1 hr to mg coral per sq ft); Shot 1 - 0.04, Shot 2 - 25, Shot 3 - 0.05, (2) Sea water (ratio of r/hr at 1 hr to ml sea water per sq ft); Shot 2 - 20, Shot 3 - 200, Shot 4 - 10, (3) Device Components (ratio of r/hr at 1 hr to fraction of device per sq ft); Shot 1 - 20×10^{12}, Shot 2 - 25×10^{12}, Shot 3 - 3×10^{12}, Shot 4 - 50×10^{12}. The constancy of these values should serve as a means of testing the reliability of sampling methods, testing the reliability of the component analysis for tracing fallout components, and, in the absence of a radioactive component (fission product surface density data), to furnish a guide as to the radiation field associated with a given surface density of debris material.

TABLE 4.3 - Distribution of Fallout Activity[a] with Particle Size
Shot 1

Sampler Location		Size Range, mm.						
		>1.9[b]	1.9-0.93	0.93-0.57	0.57-0.42	0.42-0.29	0.29-0.26	< 0.26
Love	Activity (mv)	135.0	33.06	33.67	19.69	14.58	4.08	89.23
	Wt(g)	4.542	0.662[c]	0.414[c]	0.217	0.108	0.0598	-
	Specific Activity(mv/g)	29.7	49.9	81.3	90.7	135.	68.2	-
Oboe	Activity(mv)	1.84	4.17	1.94	0.656	1.79	0.005	6.50
	Wt(g)	0.132	0.292	0.150[c]	0.0915	0.0669	0.0016	-
	Sp. Activity (mv/g)	13.9	14.3	12.9	7.17	26.8	3.13	-
Uncle	Activity(mv)	0.121	2.57	1.79	3.30	1.12	0.0814	12.46
	Weight(g)	0.083	0.188	0.715[c]	1.410	0.961	0.057	-
	Sp. Activity (mv/g)	1.47	13.7	2.50	2.34	1.16	1.43	-
William	Activity(mv)	4.70	1.12	1.31	1.12	1.65	0.024	8.19
	Weight(g)	1.704	0.406	0.198[c]	0.174	0.150	0.002	-
	Sp. Activity (mv/g)	2.76	2.76	6.60	6.45	11.0	11.80	-
Zebra	Activity(mv)	0.307	2.09	3.73	1.12	1.16	0.016	11.64
	Weight(g)	0.068	0.394[c]	0.661	0.432	0.252	0.009	-
	Sp. Activity (mv/g)	4.53	5.30	5.64	2.59	4.60	1.72	-

(a) Measured by 4π gamma chamber, 9 March 1954. 0.1 mg radium produces a reading of 78 mv.
(b) The fraction >1.9mm generally contained pieces of flour crust, mold, organic debris, etc.
(c) Analysis made for sodium content. Background amounts only detected.

	Sample 1	Sample 2	Sample 3	Sample 4
Activity remaining in the insoluble residue	76%	82%	96%	98%
Soluble activity in ionic form	23%	8%	4%	2%
Activity in colloidal form	1%	Trace	Trace	Trace

The percentages refer to the comparative counting rates of each fraction as measured with an end-window GM tube under the same geometrical conditions. These results are consistent with those found in similar studies on fallout performed at the site (see Tables 3.5 and 3.6).

Sample 1 was obtained from a DMT filter. The sample was leached in water for 3 days and was 20 days old at the beginning of the experiment.

Sample 2 was obtained from a DMT filter. The sample was leached in water for 4 weeks and was 25 days old at the beginning of the experiment.

Sample 3 consisted of several fallout particles obtained from a belt sampler.[29] The sample was leached in water for 2 weeks and was 6 1/2 months old at the beginning of the experiment.

Sample 4 consisted of several fallout particles obtained from a belt sampler. The sample was leached in water for 3 weeks and was 6 1/2 months old at the beginning of the experiment.

4.3.4 Mechanism of Formation

The processes by which the fallout particles originated can be described as follows. The material constituting the non-active body of the fallout particle was derived from the coral atoll. Modern reef building corals are composed mostly of the calcium carbonate chiefly in the form of aragonite. The effect of the bomb detonation was to heat and throw aloft a huge amount of coral dust. Most of the coral dust which was close enough to the explosion to become contaminated with radioactivity was heated sufficiently to drive off carbon dioxide and to form calcium oxide. These calcium oxide particles swept off the condensing fission products which were probably in the form of very small metallic or metallic oxide particles. At some subsequent time, as the cloud cooled, the calcium oxide hydrated to calcium hydroxide. This could easily have occurred while the particles were still in the air since large amounts of sea water were evaporated and blown into the air by the explosion. In some cases, the hydration was not complete as shown by the examples of several particles still retaining cores of unaltered calcium oxide.

Probably during the hydration process a part of the soluble fraction of the radioactive material went into solution and diffused into the particle leaving a zone of radioactivity which was most intense on the surface and diminished gradually to very low levels within a distance of about 100 μ.

At about the same time, the outer surfaces of the calcium hydroxide particles must have been carbonated by the carbon dioxide of the atmosphere. It is well known from observations on the hardening of plaster (calcium hydroxide) that the outer layer of the plaster is slowly converted to calcium carbonate in the presence of moist air. The fallout particles were exposed to moist tropical air several days before their shipment to this Laboratory. A study of the thin sections plainly showed the progressive carbonation of the calcium hydroxide which was, however, confined to a surface layer usually not exceeding 100 μ in thickness. Any calcium carbonate formed in this manner would probably have the calcite structure as this is the stable form at low temperatures. The X-ray diffraction analyses showed the presence of both calcite and aragonite (unaltered coral) in the fallout particles. However, the amount of calcite was much greater than the amount of aragonite indicating that most of the calcium carbonate in the fallout particles was of this secondary origin.

It seems probable that most of the fallout particles were formed from discrete grains of coral rather than by the agglomeration of pulverized materials. This is evidenced by the homogeneity of the particle in texture and composition, by the angular shape of the particle and by the occurrence in some particles of a central core of unaltered coral surrounded by a layer of calcium hydroxide.

A few of the particles, however, showed definite signs of being formed by accretion. They had spherical or sub-spherical shapes and were not homogeneous but were formed of agglomerations of crystalline grains and the radioactivity was distributed irregularly throughout the particle.

Some of the particles were not close enough to the fireball to be decarbonated and remained unaltered except for collecting a surface coating of radioactivity.

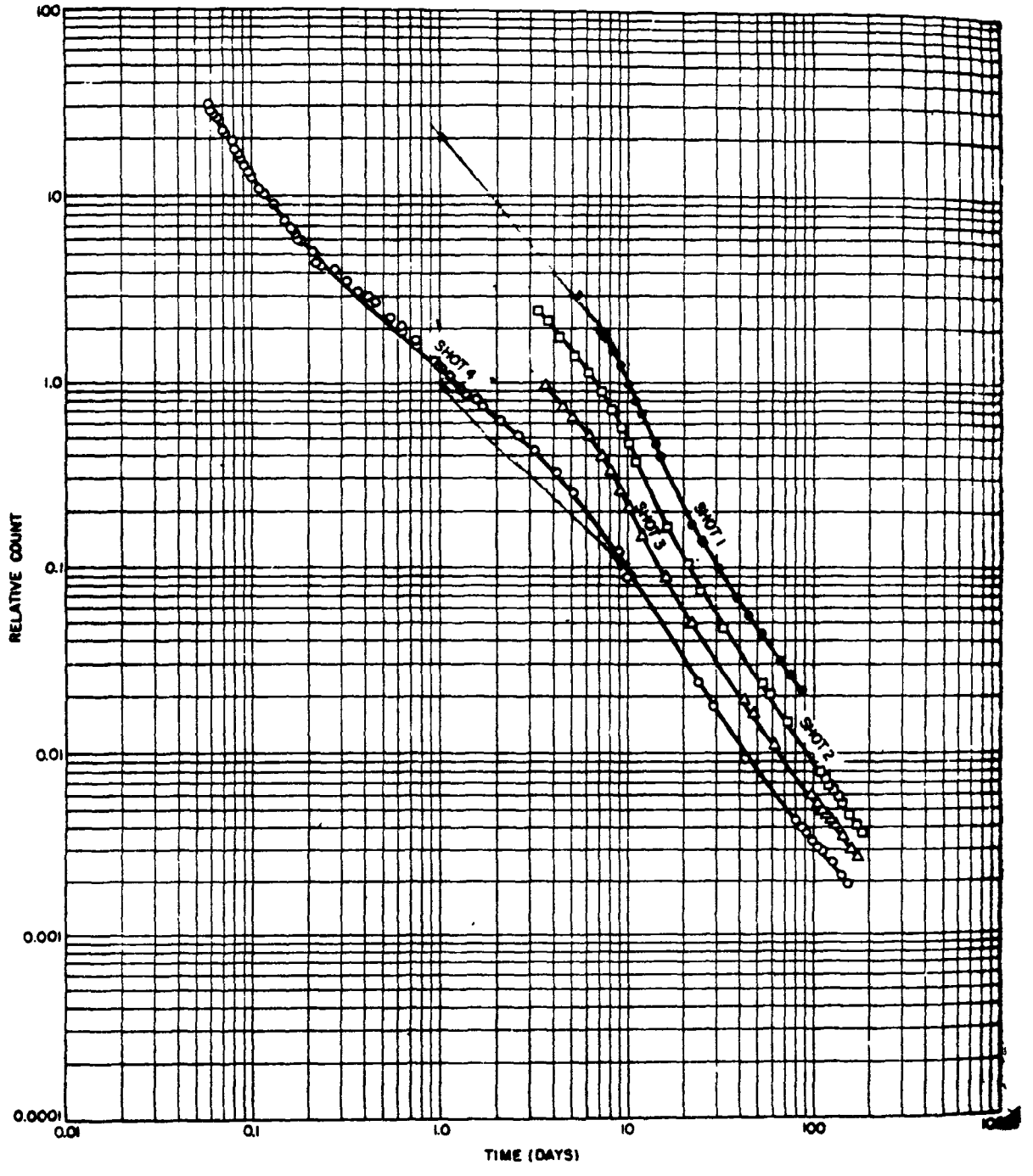

Fig. 5.1 Gross Beta Decay of Fallout Samples From Shots 1, 2, 3, and 4

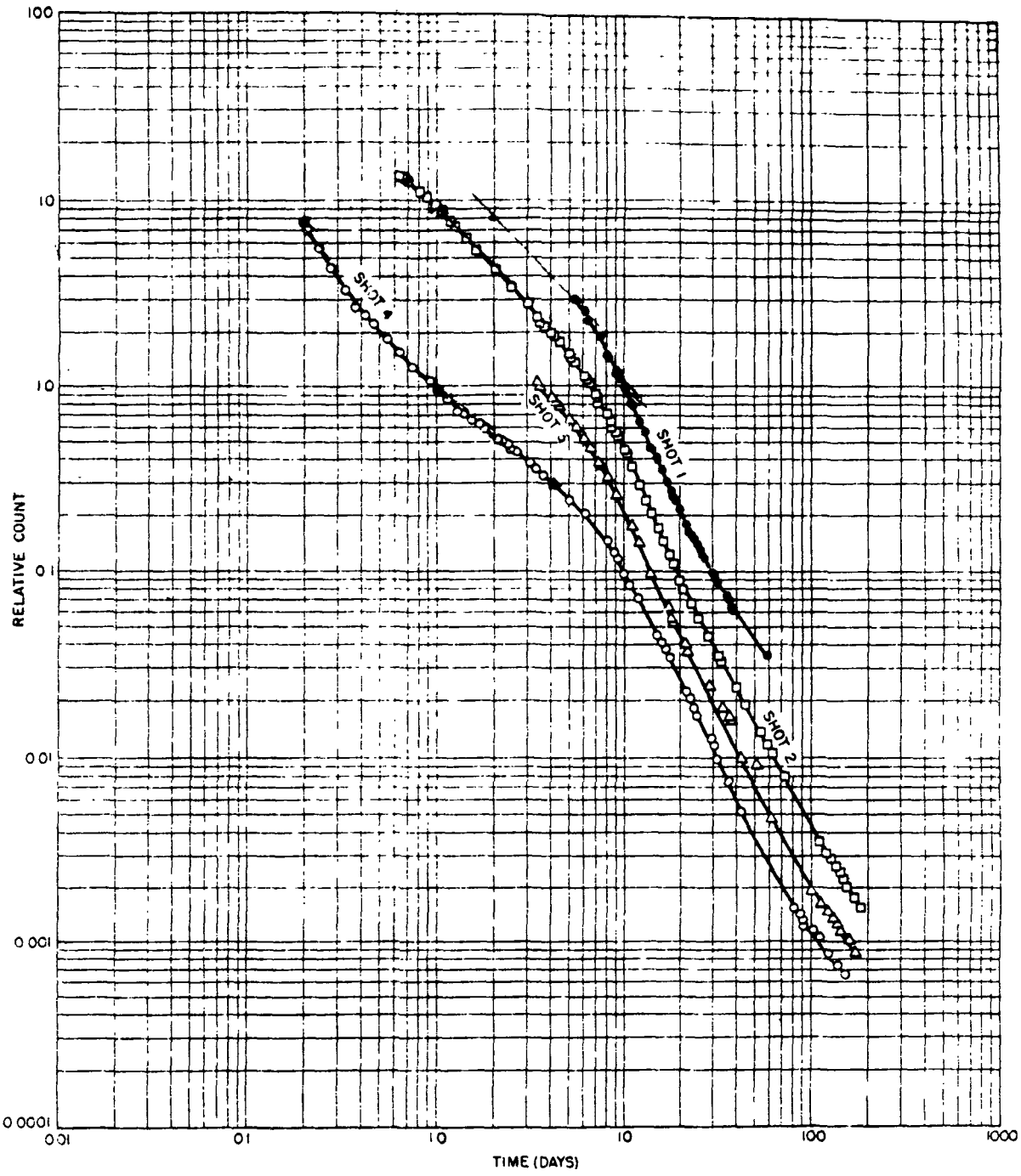

Fig. 5.2 Gross Gamma Decay of Fallout Samples From Shots 1, 2, 3, and 4

Solving Eq. 5.4 with the data from Table 5.5 for shelves 1, 2, and 3 gave the values of the constants in Eq. 5.2. Hence,

$$R^{o} = R + 2.820 \times 10^{-6}R^{2} + 1.388 \times 10^{-10}R^{3} - 6.738 \times 10^{-16}R^{4} \qquad (5.5)$$

Equation 5.5 may be expressed as,

$$R^{o}/R = 1 + y \qquad (5.6)$$

in which

$$y/R = 2.820 \times 10^{-6} + 1.388 \times 10^{-10}R - 6.738 \times 10^{-16}R^{2} \qquad (5.7)$$

These equations give an effective dead time of 200 μsec at about 4000 c/m. The value of y for each observed sample and background count was read from a plot of y against R. From + 1.5 days, + 5 days, the sample was observed on a gas-flow counter at the site and from + 9 days it was counted at USNRDL on other gas-flow counters. The ionization and beta check well from about 0.4 to 10 days; at earlier times the ionization decay was somewhat faster.

Calculated beta decay curves for Shots 1 and 4 are plotted in Fig. 5.4. The decay of the induced activities for Shot 4 are included. The calculations were based on capture to fission ratios[31] and on the fission product d/m for 10,000 fissions at zero time.[14] The experimental beta decay for Shot 4 are superimposed on the plots by normalizing the 10-day values. Agreement between the observed and calculated curves is fair. The induced activities cease to effect the gross decay at + 60 days. The calculated decay curves exhibit some differences in the mode of decay between the radioactivities produced by Shots 1 and 2 for times less than + 60 days. The observed curves are all somewhat steeper at + 60 days and longer. The gamma decay of samples from Shots 2 and 4 at times shorter than + 10 days are different. Unfortunately only single samples were available for the early time decay for those two cases; and, further, the decays were observed on counters having different spectral responses. Hence there is no basis for determining the real significance, if any, of the differences. The ionization and gamma count decay could not be expected to agree with the calculated curves as closely as the beta decay; however, their divergence generally was not great for short intervals of time.

5.1.3 Gamma Spectrometer Measurements

Since the gamma analyser was converted from an alpha analyser after Shot 1, it was not available for early measurements on fallout samples from that shot. Gamma spectra were taken of gross decay samples from Shots 2 to 4 at various times after detonation. The results are summarized in Tables 5.6 through 5.9. In these tables the heights of the various peaks are shown relative to a value of one for the energy peaks nearest 0.1 Mev.

Since a small NaI crystal was used, the spectra were limited to the lower energy region and the peak at about 0.5 Mev was undoubtedly contributed to by annihilation radiation from gammas of higher energy than 1 Mev. However, the data were used mainly to compare the general

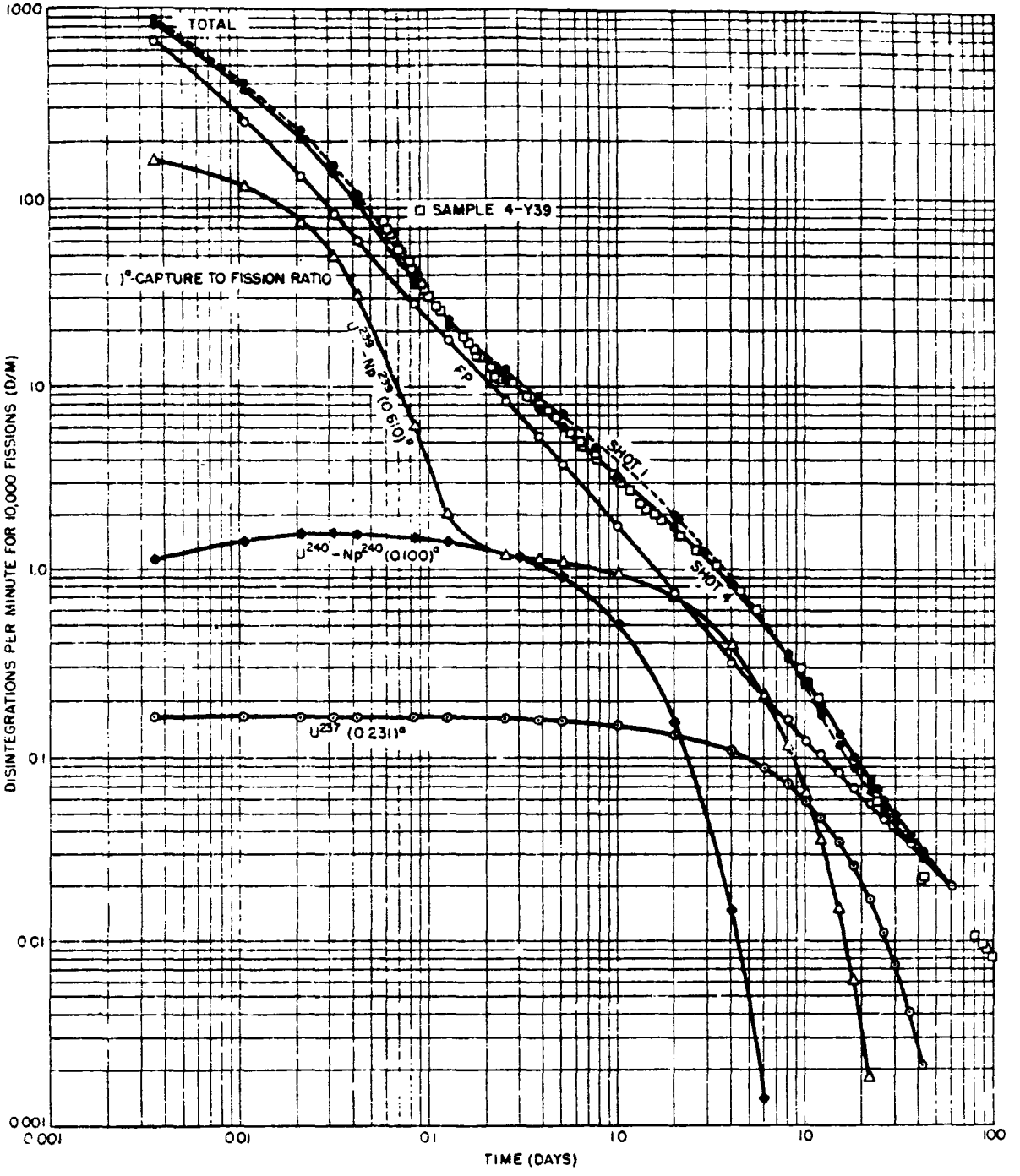

Fig. 5.4 Calculated Beta Curves

spectra from samples collected at different places and different shots with time. A comparative analysis for only one fallout sample from each shot is presented here.

5.1.3.1 Shot 1

A sample of fallout from Rongelap was analysed on + 29 and + 31 days after detonation. The results are shown in Table 5.6. Most of the same peaks show up for both curves with the exception of 0.03 and 0.27 Mev which do not appear at 31 days. Also the relative height of the 0.22 Mev curve is somewhat lower at 31 days. The 31 day curve shows a greater similarity to the other shots than the 29 day curve. In view of the fact that the calibration of the analyser was not completed at the time the first analysis was made the data collected on + 31 days are probably the more significant of the two analyses.

TABLE 5.6 - Gamma Energy Measurements from Rongelap Sample, Shot 1

Time after Shot (days)	Energy (Mev)								
	0.03	0.07	0.10	0.15	0.22	0.27	0.32	0.50	0.62
	Observed Peak Height Relative to 0.10 Mev Peak								
29	0.67	0.80	1.0	0.86	0.59	0.35	0.17	0.18	0.05
31	-	0.57	1.0	0.57	0.12	-	0.12	0.15	0.05

5.1.3.2 Shot 2

On + 2 days there are significant peaks at 0.03, 0.08, 0.23, 0.30, 0.38, 0.62.

On + 3 days, the 0.30 has dropped way down, the 0.23 is about the same, the 0.08 is considerably higher and a very high peak has shown up at 0.12 Mev along with a smaller 0.15 peak. The higher energies, 0.38 and 0.62 have decreased considerably.

On + 4 days the high peak is still 0.12 Mev, the 0.08 and 0.15 are somewhat lower, and the 0.23 is about the same. There is a 0.28 peak slightly lower than the 0.23. The higher energies are still very low.

On + 6 days the 0.03 peak is the same as it was in all previous plots. There is very little change from R + 4 days.

On + 6.25 days. Very similar to R + 6 days. The 0.08 and 0.15 peaks are now symmetrical bulges on either side of the high 0.12 peak.

On + 9 days. Same as R + 6 except the 0.03 peak does not appear.

On + 11 days. Similar to R + 9 days except 0.03 peak again appears. There is a low but definite peak at around 0.50 which has been present since + 4 days.

TABLE 5.7 - Gamma Energy Measurements from Sample 2-A5, Shot 2

Time after Shot (days)	Energy (Mev)									
	0.03	0.08	0.09	0.12	0.15	0.22	0.28	0.36	0.50	0.70
	Observed Peak Height Relative to 0.12 Mev Peak									
2	0.55	0.63	0.45	-	-	1.0	3.8	1.26	0.37	0.45
3	0.25	0.75	-	1.0	0.47	0.22	-	-	-	-
4	0.20	0.42	-	1.0	0.36	0.18	0.11	-	-	-
5	0.20	0.40	-	1.0	0.40	0.17	0.11	-	0.03	-
5.3	0.21	-	0.45	1.0	-	0.16	0.10	-	0.34	0.45
9	-	0.50	-	1.0	0.46	0.25	-	-	-	-
11	0.39	0.42	-	1.0	-	0.21	0.05	-	0.04	-

5.1.3.3 Shot 3

It appears that for this sample which was observed from + 3 days to + 15 days, the amount of low energy (less than 0.1 Mev) radiation increased with time while the high energy (greater than 0.15 Mev) fraction decreased.

There is a very prominent peak at 0.10 Mev at all times up to + 16 days.

TABLE 5.8 - Gamma Energy Measurements from Sample 3 - Coca TC,Shot 3

Time after Shot (days)	Energy (Mev)								
	0.03	0.08	0.10	0.15	0.22	0.37	0.28	0.50	0.65
	Observed Peak Height Relative to 0.10 Mev Peak								
3	0.27	0.39	1.0	-	0.16	-	0.10	0.014	-
4	0.24	0.32	1.0	-	0.22	-	0.09	0.013	0.015
5.6	0.36	0.54	1.0	-	0.19	-	0.09	0.022	0.015
6	0.28	0.29	1.0	-	0.16	-	0.09	0.02	0.01
7	0.31	0.31	1.0	-	0.18	-	0.09	0.03	0.02
8.7	0.37	0.36	1.0	-	0.18	-	0.09	0.03	0.01
9.3	0.41	0.47	1.0	-	0.22	-	0.12	0.04	0.02
10	0.36	0.36	1.0	-	0.18	0.04	-	0.04	-
11	0.42	0.45	1.0	0.21	0.12	0.05	-	0.02	-
16	0.49	0.56	1.0	0.38	0.28	0.09	-	0.09	-

5.1.3.4 Shot 4

These spectra have an unusually high component at 0.65 Mev. It was generally higher than the neighboring 0.50 Mev peak. There were few peaks below 0.06 Mev, at least up to the + 22-day curve where a 0.04 peak definitely occurs. These data do not change much with time.

TABLE 5.9 - Gamma Energy Measurements from Sample 4-Y39, Shot 4

Time after Shot (days)	Energy (Mev)											
	0.01	0.04	0.06	0.09	0.14	0.20	0.29	0.35	0.43	0.50	0.65	0.71
	Observed Peak Height Relative to 0.09 Mev Peak											
1.3	(1.57)	(1.87)	(4.0)	(1.0)	-	(0.15)	(0.13)	-	-	-	-	-
3.4	0.24	-	0.35	1.0	-	0.15	-	-	-	0.02	0.01	-
8.1	-	-	0.59	1.0	-	0.23	-	-	-	0.04	0.04	-
9.2	-	-	0.72	1.0	-	0.24	-	0.36	-	0.19	0.19	0.07
14.1	-	-	-	1.0	-	0.36	-	0.10	-	0.06	0.07	-
18.3	-	-	0.58	1.0	-	0.30	-	0.12	-	0.07	0.13	-
22.3	-	0.57	-	1.0	-	-	-	-	-	-	-	-
22.3	-	0.72	-	1.0	0.60	0.41	0.26	-	-	0.22	0.23	-

5.1.3.5 Comparisons of Spectra of Samples from Shots 1 through 4

In every curve studied the highest peak occurred at 0.09 ± 0.01 Mev. There was usually, but not always, one or more lower energy peaks near this energy. If the 0.09 Mev peak is given a relative height of 1.0, then the relative heights of the other peaks were about 0.5 for 0.01 Mev and 0.7 for 0.04 Mev. These relative heights decreased with time. There was another definite peak 0.20 Mev which ran about 0.30 of the highest peak. Higher energy peaks were observed at 0.50 and 0.65 Mev ranging from 0.1 to 0.2 of the highest peak. The 0.43 Mev peak however is doubtful since it appears in only one curve. The small NaI crystal which was used was not satisfactory for higher energies. In addition, the large amount of shielding required because of the high background at the site increased the scattering which resulted in very high counts in the low energy region and probably the peak at 0.50 Mev. The low efficiency of the crystal at the higher energies, however, was the chief reason for not taking spectra above the 1 Mev region.

The energies and relative heights of the peaks at 0.04, 0.06, 0.09, 0.20, and 0.29 Mev were very close to those observed in a pure Np^{239} spectrum which would indicate larger amounts of Np^{239} gammas. Some of these peaks gradually disappeared as the Np decayed out.

The following generalizations are evident from the analyses of the gamma spectra:

1. There did not appear to be any significant difference in the distribution of gamma-ray energies between the samples from the first four detonations.

2. The gamma analyzer curves showed no important differences between various samples from the same shot indicating that fractionation was not detectable by this method.

3. There was no great change in the relative heights of the various gamma peaks with time, although there was a detectable shift from the high 0.10 Mev peak toward both the low (0.03 Mev) and high (0.50 Mev) ends of the spectrum at later times.

4. There was a relatively large amount of 0.10 Mev gamma radiation present in the gross fallout mixture.

5. The relative peak height description permitted a general comparison of samples from different shots, from different locations for a given shot, and for the same sample at various times after burst. It should be emphasized that the descriptive technique used here, namely, analysis by relative peak height, is only a qualitative summary of the important photon energies present and has no relation whatever to the true photon-energy distribution of the radiation source.

5.1.4 Absorption Measurements

Aluminum absorption measurements were made with absorbers ranging in thickness from 0 to 3430 mg/sq cm. Before plotting, the aluminum absorber thickness was corrected for air and window thickness. Lead absorption measurements were taken with lead sandwiched between two aluminum absorbers. The aluminum absorber next to the counter window had a thickness of 1590 mg/sq cm and that just above the counting source 861 mg/sq cm. The lead absorbers ranged in thickness from 0 to 29.0 g/sq cm. The absorption measurements were taken at various times after detonation on one fallout sample from each of Shots 1 through 4.

5.1.4.1 Lead Absorption

A summary of gamma ray energies from the lead absorption curves is given in Table 5.10. These curves were analyzed into three components which give the "apparent" gamma energies although it is known that there are many different gammas contributing. The soft, medium, and hard components were then used to compare different samples with each other. The amount of each component was corrected by the counter efficiency for the apparent energy. The usual procedure of analyzing absorption curves was used; the "zero absorber" count rate was determined by extrapolating the three lines on a semilog plot to zero absorber thickness. The energy of each line was determined from Pb half-thickness curves; this energy was used to determine, from Fig. 2.1, the component crystal efficiency which was, in turn, used to weight the "zero absorber" count rate for each component to determine the relative amount of that component.

From these data the following conclusions may be drawn:

(1) Between 0.3 and 26 days there appeared to be no appreciable change in the energy of the soft gamma component. The average energy for all soft gammas observed was 0.16 Mev with a maximum deviation of 0.04 Mev.

(2) Between 0.3 and 26 days there appeared to be no significant change in the energy of the medium gamma component. The average energy for all medium gammas observed was 0.37 Mev with a maximum deviation of 0.11 Mev.

(3) There were larger variations in the energies of the hard gammas with respect to time especially for Shots 2 and 3. However, no definite trend is apparent as may be seen from Table 5.11 where the hard gamma component has been averaged for each shot. The over-all hard gamma energy average was 1.3 Mev with a maximum deviation of 0.5 Mev.

(4) There appears to be no trend common to all shots for the

TABLE 5.10 - Energies and Gross Distribution of Gamma Rays from Gross Fallout Samples

Shot Sample	Time After Burst (days)	Low Energy Gammas		Medium Energy Gammas		High Energy Gammas	
		Energy (Mev)	Amount (%)	Energy (Mev)	Amount (%)	Energy (Mev)	Amount (%)
Shot 1							
1-251.03	3.77	0.16	42	0.32	29	1.1	29
" "	4.52	0.20	41	0.36	21	1.1	38
" "	3.35	0.17	46	0.30	27	1.0	27
" "	4.39	0.16	30	0.29	32	1.1	38
" "	4.73	0.18	47	0.38	23	1.5	30
" "	5.22	0.16	22	0.30	33	1.2	45
" "	3.85	0.14	48	0.32	21	1.15	31
" "	4.81	0.15	37	0.33	24	1.25	39
" "	6.20	0.20	32	0.48	17	1.3	51
" "	6.52	0.16	24	0.33	18	1.3	58
Shot 2							
Elmer	4.47	0.16	44	0.44	22	1.20	34
2-A5	3.78	0.17	66	0.40	16	1.80	18
"	3.19	0.13	68	0.48	15	1.5	17
"	4.07	0.165	62	0.40	16	1.70	22
Shot 3							
3-Coca T.C.	4.03	0.165	53	0.37	19	1.3	28
" "	3.02	0.16	71	0.38	12	1.35	17
" "	4.17	0.17	59	0.44	15	1.45	26
" "	4.29	0.16	47	0.36	21	1.25	32
" "	4.75	0.17	49	0.38	20	1.5	31
" "	(5.13)	0.145	40	0.34	36	1.4	35
" "	6.45	0.17	37	0.42	18	1.6	45
Shot 4							
4-YAG-39	3.29	0.145	50	0.34	23	1.2	27
Plane Wipe	0.29	0.15	26	0.40	13	1.2	61
" "	1.63	0.16	38	0.34	19	1.0	43
" "	2.37	0.15	35	0.42	26	1.05	39
" "	2.67	0.135	35	0.31	27	1.2	38
" "	3.35	0.16	34	0.39	25	1.1	41
" "	5.13	0.135	36	0.29	29	1.0	35

variation of the proportion of different gamma components with respect to time after burst. The average percentages for the low, medium, and high energy gamma rays was 45, 22, and 35 per cent, respectively. However, the percentages varied considerably from one absorption curve to another. The lead absorption curves of 1-251.03 sample taken on + 22.4 and + 26.1 days show an exceptionally large proportion of high energy gammas.

TABLE 5.11 - Average Hard Gamma Energy for Each Shot

Shot	Average Gamma Energy (Mev)	Maximum Deviation (Mev)
1	1.2	± 0.2
2	1.55	± 0.35
3	1.41	± 0.19
4	1.11	± 0.11

Table 5.12 shows the percentage of each gamma component and their averaged energy for each shot at times less than 14 days.

TABLE 5.12 - Average Energy and Average Percentage of "Apparent" Gamma Components for each Shot at Times Less than 14 Days

Shot	Soft Gamma (%)	Max. Dev. (%)	Med. Gamma (%)	Max. Dev. (%)	Hard Gamma (%)	Max. Dev. (%)	Average Energy (Mev)
1	39	± 15	25	± 8	36	± 9	0.59
2	60	± 16	17	± 5	23	± 11	0.52
3	50	± 20	20	± 16	30	± 14	0.58
4	36	± 14	23	± 10	41	± 20	0.60

5.1.4.2 Aluminum Absorption

The only portion of the aluminum absorption curves analyzed was that for the highest beta energy. The upper portion of this high energy curve must be extrapolated over a large range of absorber thickness which would make any further analysis of the original curve doubtful. Analyses of aluminum absorption data for beta energies for all shots indicate that the energy of the hardest beta ray decreases with time in accordance with the theory.

The energies of the hard betas from Shots 1, 3, and 4 are listed in Table 5.13. The values for the maximum beta energy are nearly constant and approximate 2 Mev. The hard beta energy for sample 1-251.03 at later times appeared to be somewhat high compared to the samples from other shots. The beta-gamma ratio is 2 for most of the aluminum absorption curves although for Shot 3 at + 10.3 days the value was one and for one sample from Shot 4 at + 11.1 hr it was three.

TABLE 5.13 - Preliminary Summary of Beta Energies

Shot	Sample	Time after Burst	Max. Beta Energy (Mev)	Approximate Beta-Gamma Ratio(a)
1	251.03	10.2 days	2.1	2
1	251.03	14.05 days	1.3	2
1	251.03	22.15 days	1.9	2
1	251.03	26.1 days	2.2	1.5
3	Coca-TC	3.63 days	1.9	2
3	Coca-TC	4.63 days	1.85	2
3	Coca-TC	10.29 days	1.2	1
4	Y39	5.6 hr	2.6	2
4	Y39	11.1 hr	2.3	3
4	Y39	23.7 hr	2.3	2
4	Y39a	2.62 days	2.1	2
4	Y39a	3.53 days	2.0	2
4	Plane-wipe	8 hr	2.4	2
4	Plane-wipe	3.3 days	1.8	2

(a) Ratio of beta count rate to gamma count rate corrected for counter efficiency.

5.2 FISSION PRODUCT DETERMINATIONS

Radiochemical analyses of the fission produced radionuclides Sr^{89}, Y^{91} Zr^{95}, Zr^{97}, Mo^{99}, Ag^{111}, Cd^{115}, Ce^{141}, Ce^{144}, Nd^{147}, Pm^{149}, Sm^{153}, Eu^{156}, Gd^{159}, and Tb^{161} were performed.

5.2.1 Radiochemical Procedures

Radiochemical determinations of the fission products were made according to standard published procedures[7] which are outlined here.

Sr^{89} was separated as the nitrate and purified by scavenging precipitations. It was determined as the carbonate.

Y^{91} was separated as the fluoride, purified by ion exchange, and determined as the oxalate.

Zr^{95} and Zr^{97} were exchanged with carrier Zr by use of HF, purified by scavenging precipitations and determined as the oxide.

Mo^{99} was separated and purified as the alpha-benzoin oximate. It was determined as $PbMoO_4$.

Ag^{111} was separated, purified, and determined as the chloride.

Cd^{115} was separated as the sulfide and purified by scavenging. It was determined as $CdNH_4PO_4$.

Ce^{141} and Ce^{144} were separated as the iodate, purified by scavengings, and determined as the oxalate.

Yields of various fission product radionuclides were determined relative to the yield of Mo^{99} and/or Zr^{95}. The determinations were made on different samples collected at various distances from ground zero. Comparison of relative yields among these reveals the extent of fractionation which occurred. In the absence of appreciable fractionation the relative amount of any fission product nuclide of interest is then obtainable from the measured fission yield curve.

5.2.2 Results

Analyses were made on all adequate samples obtained from the various events. The radiochemical results are presented in the form of R values where R is defined as follows:

$$R = \frac{C_r'}{C_x'} \Big/ \frac{C_r}{C_x}$$

where C_r' = counting rate at zero time of reference radionuclide in uranium thermal neutron fission.

C_x' = counting rate at zero time of radionuclide of interest in uranium thermal neutron fission.

C_r = counting rate at zero time of reference radionuclide in event of interest.

C_x = counting rate at zero time of radionuclide of interest in event of interest.

Counting rates of a given radionuclide from the event of interest were measured under the same conditions of geometry and absorption as those used in measurements in thermal neutron fission. Counting rates were corrected for chemical yield. By inspection it is seen that an R value of 1 shows a relative fission yield the same as in thermal neutron fission of uranium, a value of greater than 1 shows a higher relative yield and one of less than 1 shows a lower relative yield. Results of the measurements are given in Table 5.14. The precision of measurement was 10 per

cent or better. Results of analyses on cloud samples are included to allow comparisons between fallout and cloud material. The cloud samples were portions of filter paper collections made for radiochemical determinations of weapon yield by LASL and UCRL.

5.2.3 Fractionation

5.2.4 Fission Yield Curves

5.3 INDUCED ACTIVITIES

Analyses for Na^{24}, K^{42}, Mg^{28}, Cl^{38}, Np^{239}, U^{237}, and U^{240} were performed on cloud and fallout samples. However, because of the difficulty of obtaining early samples only Na^{24}, Np^{239}, U^{237}, and U^{240} were detected. The fallout samples analyzed at the site were aliquoted as described in Section 3.1. The remainder of these samples and the cloud samples were analyzed at USNRDL.

5.3.1 Radiochemical Procedures

Radiochemical determinations were made according to either standard published procedures[21] or those developed at USNRDL. They are outlined here and described more fully in Appendix A.

Na^{24} was separated from the gross activity by a two-step procedure. First, the alkali metal fraction was separated from the gross activity by ion exchange. Then, Na^{24} was isolated by a gravimetric procedure employing the specific precipitation of sodium zinc uranyl

Pg. 122 Deleted.

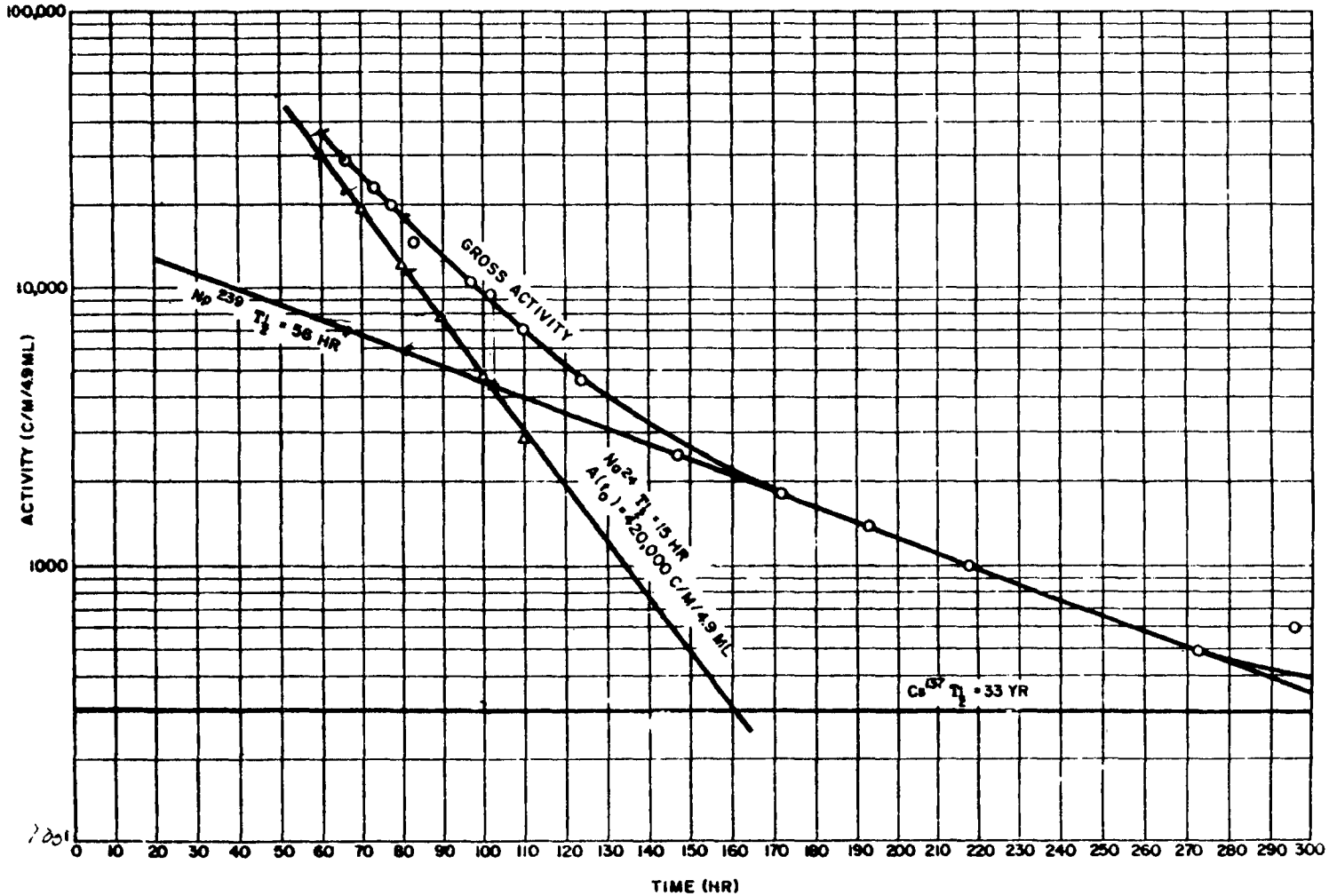

Fig. 5.5 Decay Curve of Na^{24} Sample from Shot 2. Sample was Collected 51 Nautical Miles from Ground Zero on Bearing 330°T

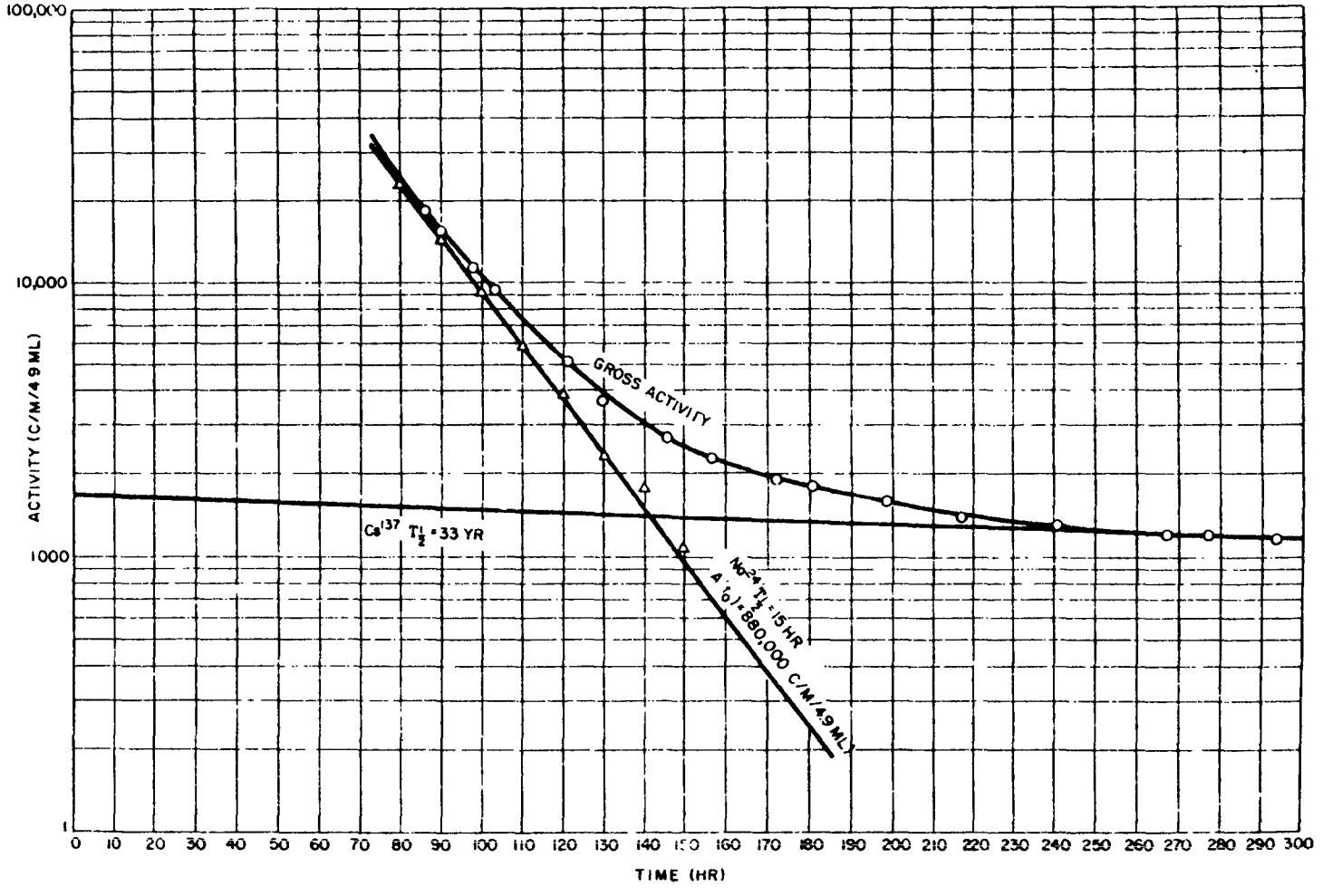

Fig. 5.6 Decay Curve of Na^{24} Sample from Shot 3. Sample was Collected at Coca Head 6 Nautical Miles from Ground Zero on Bearing 7°T

BIBLIOGRAPHY

1. Adams, C.E., Poppoff, I.C. and Wallace, N.R.
The Nature of Individual Radioactive Particles I. Surface and Underground ABD Particles from Operation JANGLE
U.S. Naval Radiological Defense Laboratory Report
USNRDL-374, November 1952 (SECRET)

2. Adams, C.E.
The Nature of Individual Radioactive Particles II. Fallout Particles from M-Shot Operation IVY
U.S. Naval Radiological Defense Laboratory Report
USNRDL-408, July 1953 (SECRET)

3. Adams, C.E.
The Nature of Individual Radioactive Particles IV. Fallout Particles from the First Shot, Operation CASTLE
U.S. Naval Radiological Defense Laboratory Report
USNRDL-TR-26, January 1955 (SECRET)

4. Ballou, N.E. and Bunney, L.R.
Nature and Distribution of Residual Contamination, II
JANGLE Project 2.6c-2 Report
WT-397 (in WT-373) June 1952 (SECRET)

5. Bigger, M.M., Rinnert, H.R., Sherwin, J.C., Kawahara, F.K. and Lee, H.
Field Effectiveness Tests of a Washdown System on an Aircraft Carrier
U.S. Naval Radiological Defense Laboratory Report
USNRDL-416, June 1953 (CONFIDENTIAL)

6. Conway, J.C. and Moore, M.F.
Spectrographic Analysis of Radioactive Materials
Analytical Chemistry, 24:463-464 (1952)

7. Coryell, C.D. and Sugarman, N. (Editors)
"Radiochemical Studies: The Fission Products, National Nuclear Energy Series", Div. IV
Vol. 9, McGraw-Hill, New York, 1951

8. "Effects of Atomic Weapons, The"
U.S. Government Printing Office
Washington, D.C., 1950

9. Farlow, N.H.
A Physico-Chemical System for Water Aerosol Measurement
U.S. Naval Radiological Defense Laboratory Report
USNRDL-TR-49, May 1955

10. Gevantman, L.H., Pestaner, J.F., Singer, B. and Sam, D.
Decontaminability of Selected Materials: Decontamination by Spraying with and Immersion in Liquid
U.S. Naval Radiological Defense Laboratory Report
USNRDL-TR-13, August 1954 (CONFIDENTIAL)

11. Greendale, A.E. and Ballou, N.E.
Physical State of Fission Product Elements Following Their Vaporization in Distilled Water and Sea Water
U.S. Naval Radiological Defense Laboratory Report
USNRDL-436, February 1954

12. Heidt, W.B., Jr., LCDR, USN, Schuert, E.A., Perkins, W.W. and Stetson, R.L.
Nature, Intensity and Distribution of Fallout from M-Shot, Operation IVY
IVY Project 5.4a Report, April 1953 (SECRET RESTRICTED DATA)
WT-615

13. Honma, M.
Flame Photometric Apparatus for Determination of Radioactive Materials
Paper presented at Amer. Chem. Society Meeting September 11, 1955
Minneapolis, Minnesota

14. Hunter, H.F. and Ballou, N.E.
Fission-Product Decay Rates
Nucleonics, 9: No. 5, C1-7 (1951)

15. Johnstone, C.W.
A New Pulse Analyzer Design
Nucleonics, 11: No. 1, 36-41 (1953)

16. LaRiviere, P.D. and Ichiki, S.K.
Autoradiographic Method for Identifying Beta-Active Particles in a Heterogeneous Mixture
Nucleonics, 10: No. 9, 22-24 (1952)

17 Laurino, R.K., Poppoff, I.G.
Contamination Patterns at Operation JANGLE
U.S. Naval Radiological Defense Laboratory Report
USNRDL-399, April 1953 (SECRET RESTRICTED DATA)

18. Macdonald, D. and Zigman, P.E.
Influence of Surface Roughness on Contamination and Decontamination Behavior of Materials
U.S. Naval Radiological Defense Laboratory Report
USNRDL-415, September 1953 (SECRET)

19. Maxwell, C.R., et al
Nature and Distribution of Residual Contamination, I
JANGLE Project 2.6c-1 Report
WT-386 (in WT-373), June 1952 (SECRET RESTRICTED DATA)

20. Maxwell, R.D.
Radiochemical Studies of Large Particles
JANGLE Project 2.5a-3 Report
WT-333 (in WT-371), April 1952 (SECRET RESTRICTED DATA)

21. Meinke, W.E.
Chemical Procedures Used in Bombardment Work at Berkeley
University of California Radiation Laboratory Report
UCRL-432, August 1949

22. Miller, C.F., Cole, R. and Heiman, W.J.
An Investigation of Synthetic Contaminants for an Atomic Burst in Deep Sea Water
U.S. Naval Radiological Defense Laboratory Report
USNRDL-411, August 1953 (SECRET RESTRICTED DATA)

23. Miller, C.F., Cole, R., Heiman, W.J. and Nuckolls, M.J.
Decontamination of Fission Products and Other Atomic Bomb Detonation Debris
U.S. Naval Radiological Defense Laboratory Report
USNRDL-439, November 1953 (CONFIDENTIAL)

24. Cole, R., Heiman, W.J., Miller, C.F.
Effect of Harbour Bottom Material on the Decontamination of Various Elements in a Synthetic Sea Water Contaminant
U.S. Naval Radiological Defense Laboratory Report
USNRDL-TR-43, February 1955 (CONFIDENTIAL)

25. Poppoff, I.G., et al
Fallout Particles Studies
JANGLE Project 2.5a-2 Report
WT-395 (in WT-371) April 1952 (SECRET RESTRICTED DATA)

26. Quan, J.T.
A Split-Image Film Comparator for X-ray Diffraction Powder
Review of Scientific Instruments, 25: No. 4 (1954)

27. Schmidt, A.C. and Wiltshire, L.L.
A Constant Flow Suction Unit for Aerosol Sampling Work
American Industrial Hygiene Association Quarterly, 16:2 June 1955

28. Spence, R.E.
Letter; LASL, J-11-96, WET 54-406D, August 6, 1954

29. Stetson, R.L., Schuert, E.A., Perkins, W.W., Shirawasa, T.H. and Chan, H.K.
Distribution and Intensity of Fallout at Operation CASTLE
CASTLE Project 2.5a Report (SECRET RESTRICTED DATA)
WT-915

30. Sverdrup, H.U., Johnson, M.W. and Fleming, R.H.
"The Oceans, Their Physics, Chemistry and General Biology"
Prentice-Hall, New York, 1942

31. Transmittal of CASTLE Device Data
Document T.U. 13-54-106S, 4 May 1954 (SECRET RESTRICTED DATA)

32. Werner, L.B.
Contamination-Decontamination Phenomenology
JANGLE Project 6.2 Report
WT-400 (Ch. 8) June 1952 (SECRET)

33. Wittman, J.P., and Goodale, T.C.
An Automatic Water Drop Collector for Field Use
Bulletin of the American Meteorological Society
Vol. 36, No. 2, February, 1955